**Supplementary Information Appendix for:**

# Real-time observation of DNA target interrogation and product release by the RNA-guided endonuclease CRISPR Cpf1

Digvijay Singh[a], John Mallon[b], Anustup Poddar[a], Yanbo Wang[a], Ramreddy Tippana[c], Olivia Yang[a], Scott Bailey[a, b] and Taekjip Ha[a, c-e]

[a]Department of Biophysics and Biophysical Chemistry, Johns Hopkins University School of Medicine, Baltimore, Maryland 21205, USA.

[b]Bloomberg School of Public Health, Johns Hopkins University School of Medicine, Baltimore, Maryland 21205, USA.

[c]Department of Biophysics, Johns Hopkins University, Baltimore, Maryland 21218, USA.

[d]Department of Biomedical Engineering, Johns Hopkins University, Baltimore, Maryland 21205, USA.

[e]Howard Hughes Medical Institute, Baltimore, Maryland 21205, USA.

**This document includes:**

**Section 1 (S1) containing Figures S1-S18 and Tables S1-S5**

**Section 2 (S2) containing additional details about materials and methods.**

# S1. Additional Results Figures

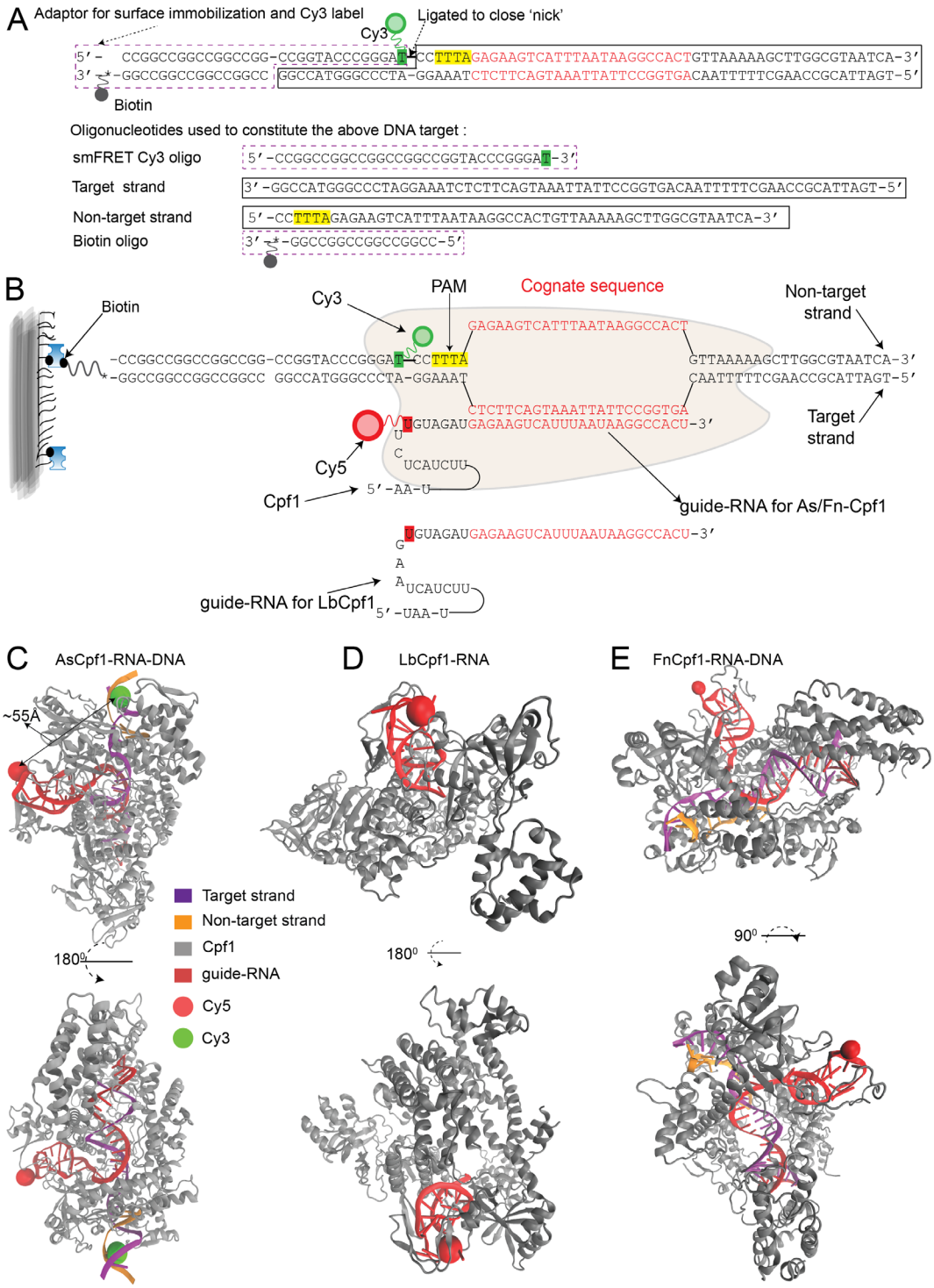

**Figure S1.** Design of DNA targets and guide-RNA along with FRET probes labeling locations in the Cpf1-RNA-DNA complex for smFRET assay for DNA interrogation by Cp1-RNA.

(*A*) Description of single-stranded DNA oligonucleotides with appropriate modifications for constitution of a fully duplexed DNA target for use in the smFRET assay. Oligonucleotides referred to as smFRET Cy3 oligo and Biotin oligo provide donor label for the smFRET assay and anchor for surface immobilization of the fully duplexed DNA target respectively. These oligonucleotides were same for all DNA targets. Other two strands were unmodified oligonucleotides, and strand that hybridizes with the guide-RNA (of Cpf1-RNA) is referred to as target strand and strand complementary to the target strand is called non-target strand. Base sequence of the target and non-target strands were changed to create DNA targets with mismatches against fixed guide-RNA sequence. These smFRET experiments were done both with DNA targets with 'nick' close to PAM at the indicated location and with DNA targets where this nick was ligated to close it. (*B*) Illustrated schematic of a complete Cpf1-RNA-DNA (b; As/FnCpf1-RNA-DNA and LbCpf1-RNA-DNA) complex showing base-pairing between different components. Sequences written in red denote cognate sequence in the DNA target and complementary sequence in the guide-RNA. (*C*) Fluorescent (Cy3 and Cy5) labeling locations shown in structure of AsCpf1-RNA bound to cognate DNA target (PDB ID: 5B43)(1). As mentioned, strand which hybridizes with guide-RNA to form RNA-DNA heteroduplex is referred to as the target strand while the other strand, containing the PAM (5'-YTN-3'), is the non-target strand. (*D*) Cy5 labeling location shown in structure of LbCpf1-RNA complex (PDB ID: 5ID6)(2). (*E*) Cy5 labeling location shown in structure of FnCpf1-RNA-DNA complex (PDB ID: 5MGA)(3).

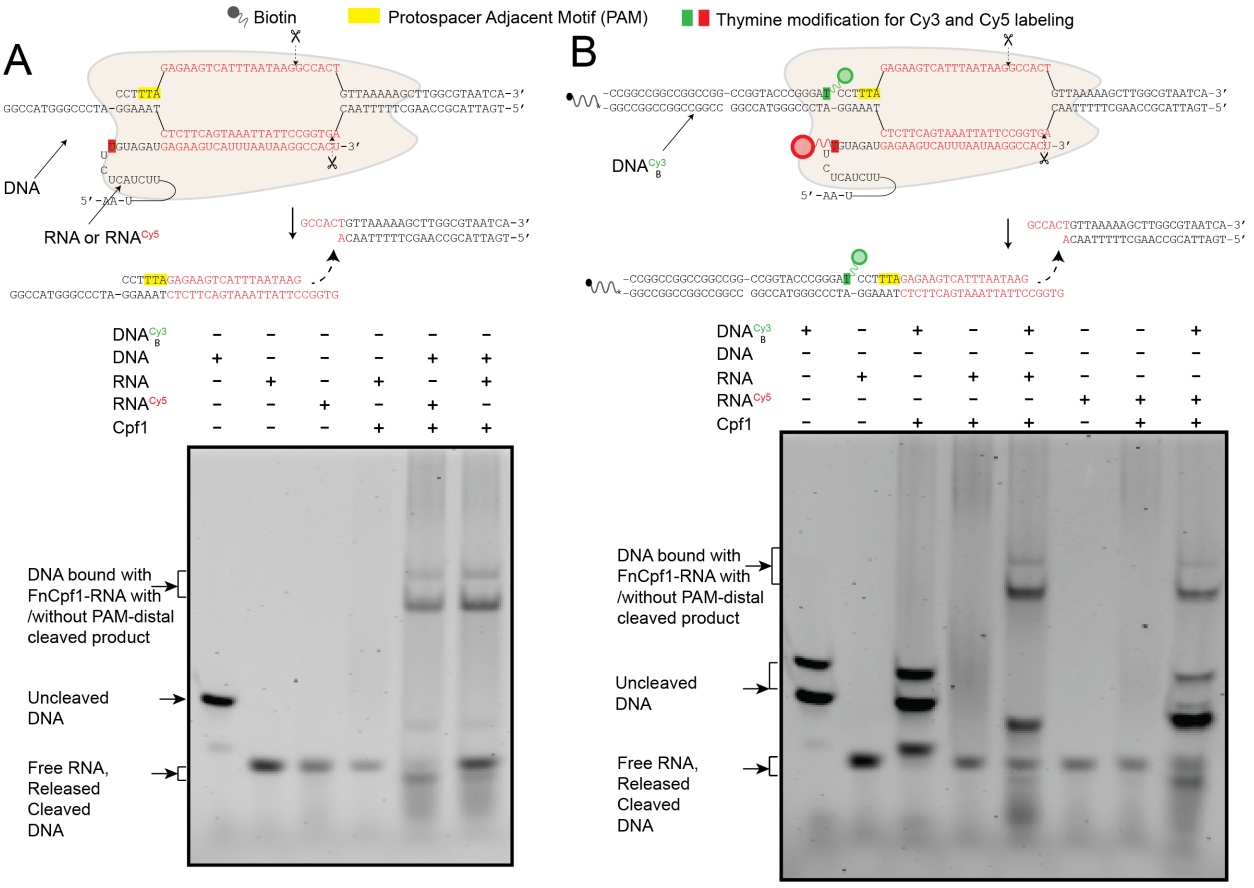


**Figure S2.** FnCpf1-RNA activity is not impaired by fluorescent labeling of guide-RNA and DNA target. FnCpf1-RNA induced DNA cleavage & binding analyzed by 4% native agarose gel electrophoresis and visualization of SYBR Gold II stained nucleic acids. (*A*) Activity of unmodified RNA and Cy5 labeled RNA for FnCpf1-RNA targeting of cognate DNA target without Cy3 or Biotin label. (*B*) Activity of unmodified RNA and Cy5 labeled RNA for FnCpf1-RNA targeting of cognate DNA target labeled with Cy3 and Biotin. It must be noted that the strands used to constitute dsDNA target with and without Cy3 and Biotin label were mixed with excess of non-target strand to ensure a near 100% hybridization of target strand with non-target strand, which results in multiple bands for the DNA substrate.

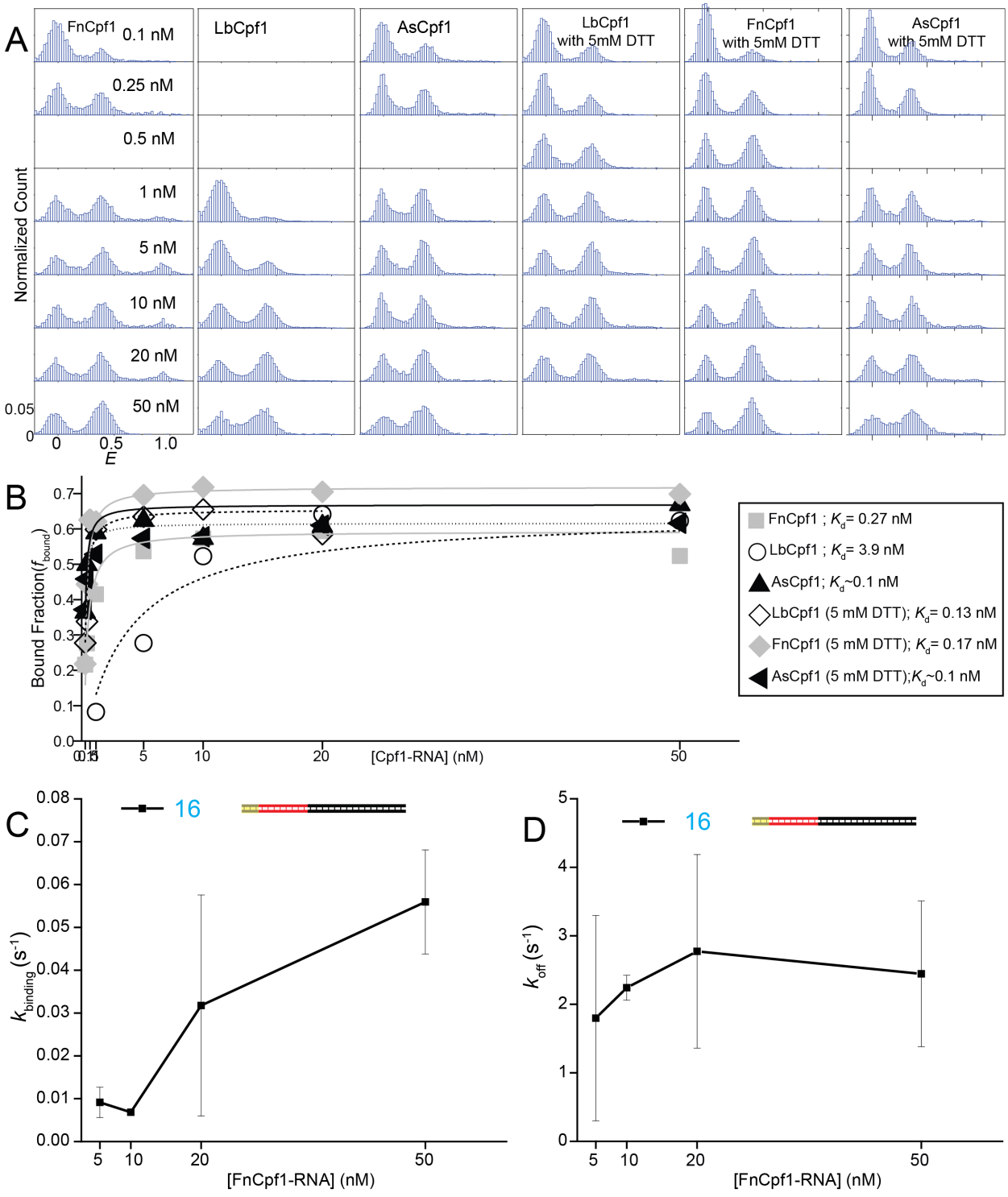


**Figure S3.** Bound fraction and rates of FRET appearance and disappearance with increasing Cpf1-RNA concentration.

(*A*) *E* histograms demonstrating increase in Cpf1-RNA bound state population of cognate DNA targets

with increasing Cpf1-RNA concentration for different Cpf1 orthologs. The third peak at high FRET efficiencies occurred only some experiments and was the result of fluorescent impurities likely due variations in PEG passivation, and they were difficult to exclude in automated analysis. (*B*) Cpf1-RNA bound fraction defined as a fraction of population of DNA target molecules with FRET (>0.2 & <0.6) vs. Cpf1-RNA concentration. Trend was fit to obtain disassociation constant ($K_d$) of Cpf1-RNA and DNA interaction. (*C, D*) After a hidden Markov analysis(4) on smFRET time-trajectories, bound and unbound states were divided based on the FRET values via thresholding at FRET= 0.2. The FRET states > 0.2 were taken as putative bounds states. Dwell-times of bound states were used to estimate the overall bound state lifetime, inverse of which was taken as FnCpf1-RNA-DNA dissociation rate ($k_{off}$). The dwell-times of the unbound states were used to estimate rate of FnCpf1-RNA and DNA association ($k_{binding}$). (*C*) The rate of binding for DNA target with $n_{PD}$ =16 showing a linear increase with the increasing concentration of FnCpf1-RNA. (*D*) The rate of FnCpf1-RNA-DNA dissociation for DNA target with $n_{PD}$ =16 remained largely unchanged at different FnCpf1-RNA concentrations. 5 mM DTT was used for (C-D) experiments. Error bars represent s.d for replicate experiments. Number of PAM-distal mismatches ($n_{PD}$) is shown in cyan.

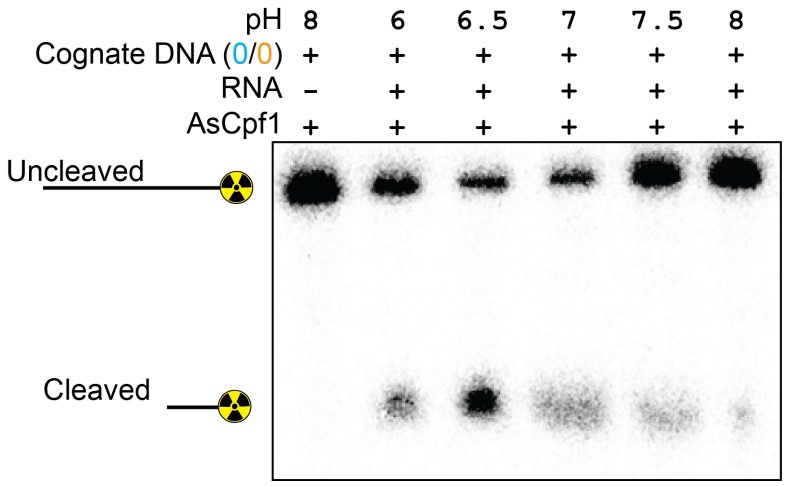


**Figure S4.** Cleavage activity of AsCpf1 at different pH conditions.

Number of PAM-distal mismatches ($n_{PD}$) is shown in cyan.

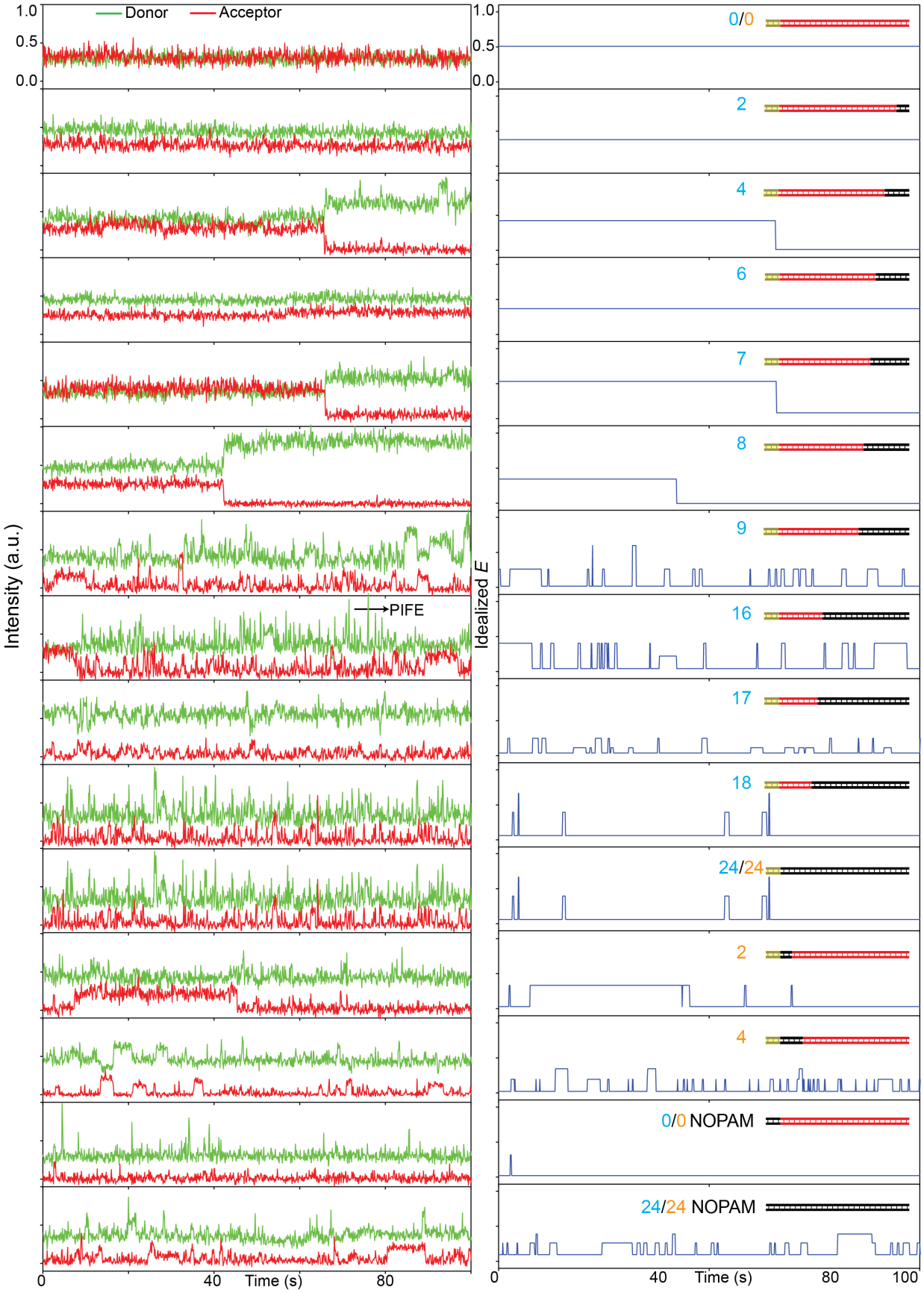
Donor
Acceptor
1.0
0.5
0.0
Intensity (a.u.)
PIFE
0
40
Time (s)
80
Idealized E
0/0
2
4
6
7
8
9
16
17
18
24/24
2
4
0/0 NOPAM
24/24 NOPAM
0
40
Time (s)
80
100

**Figure S5.** Representative smFRET time-trajectories from smFRET experiments to study DNA interrogation by AsCpf1-RNA.

These representative smFRET time- trajectories (left) along with their idealized FRET values (right) are taken from representative DNA targets with/without nick near the PAM (**Fig. S1**) and no differences were observed between them. The indicated protein induced fluorescence enhancement (PIFE) on the donor only signal is likely resulting from non-specific interaction of free-excess of Apo AsCpf1 with the DNA and was observed for all the DNA targets. Number of PAM-distal ($n_{PD}$) and PAM-proximal mismatches ($n_{PP}$) are shown in cyan and orange respectively.

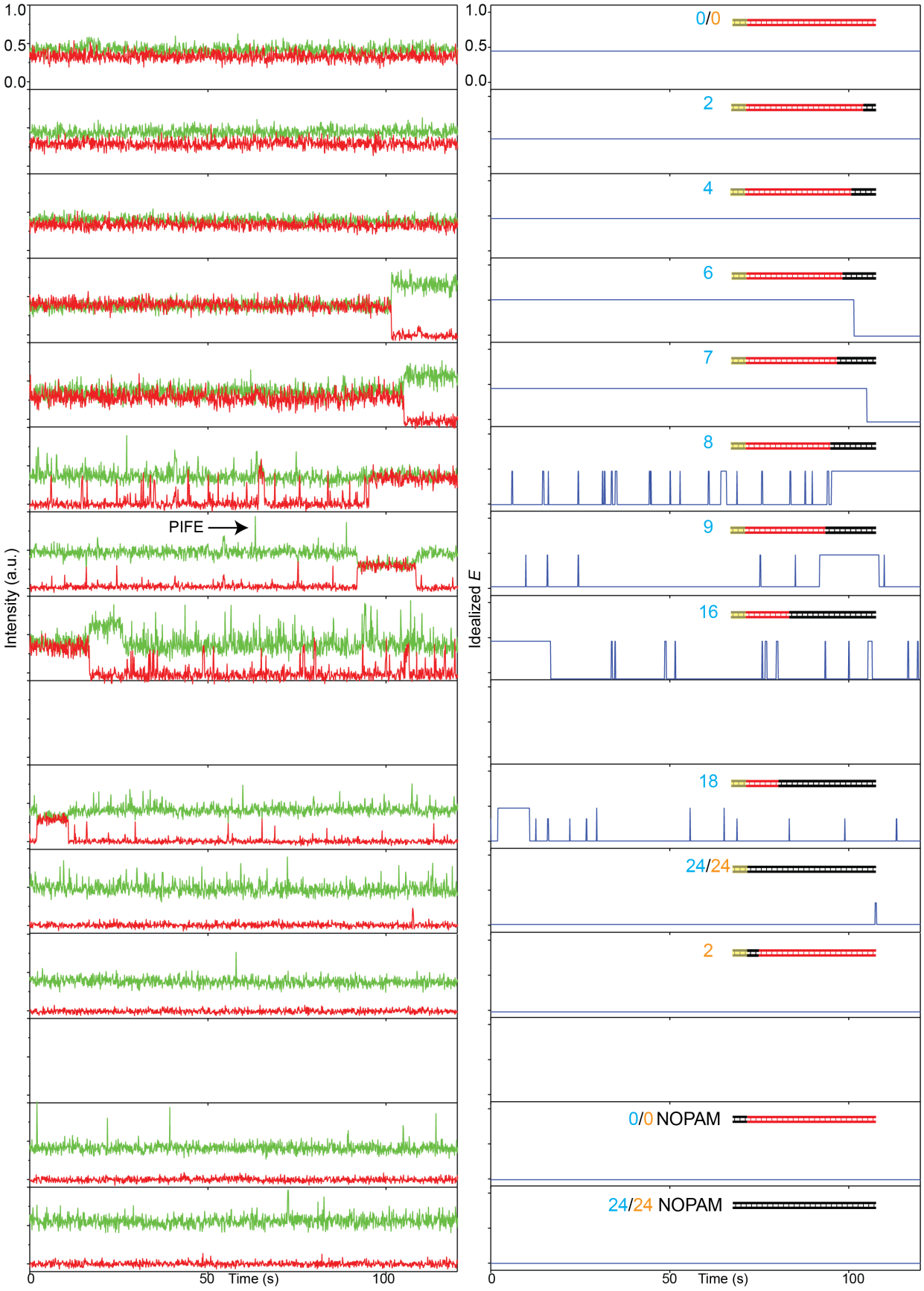
1.0
0.5
0.0
Intensity (a.u.)
PIFE
0
50
Time (s)
100
Idealized E
0/0
2
4
6
7
8
9
16
18
24/24
2
0/0 NOPAM
24/24 NOPAM

**Figure S6.** Representative smFRET time-trajectories from smFRET experiments to study DNA interrogation by FnCpf1-RNA.

These representative smFRET time- trajectories (left) along with their idealized FRET values (right) are taken from representative DNA targets with/without nick near the PAM (**Fig. S1**) and no differences were observed between them. The indicated protein induced fluorescence enhancement (PIFE) on the donor only signal is likely resulting from non-specific interaction of the free-excess of Apo FnCpf1 with the DNA and was observed for all the DNA targets. DNA targets with nick (**Fig. S1**) exhibit stronger anti-correlation between donor and acceptor signal for transient FRET binding events. PIFE upon the FnCpf1-RNA binding can influence this anti-correlation and slightly different levels of PIFE on Cy3 in DNA target with and without nick i.e. different flexibilities could be causing these variations. Photophysics or isomerization of Cy3 resulting PIFE is guided by local DNA flexibility(5). Number of PAM-distal ($n_{PD}$) and PAM-proximal mismatches ($n_{PP}$) are shown in cyan and orange respectively.

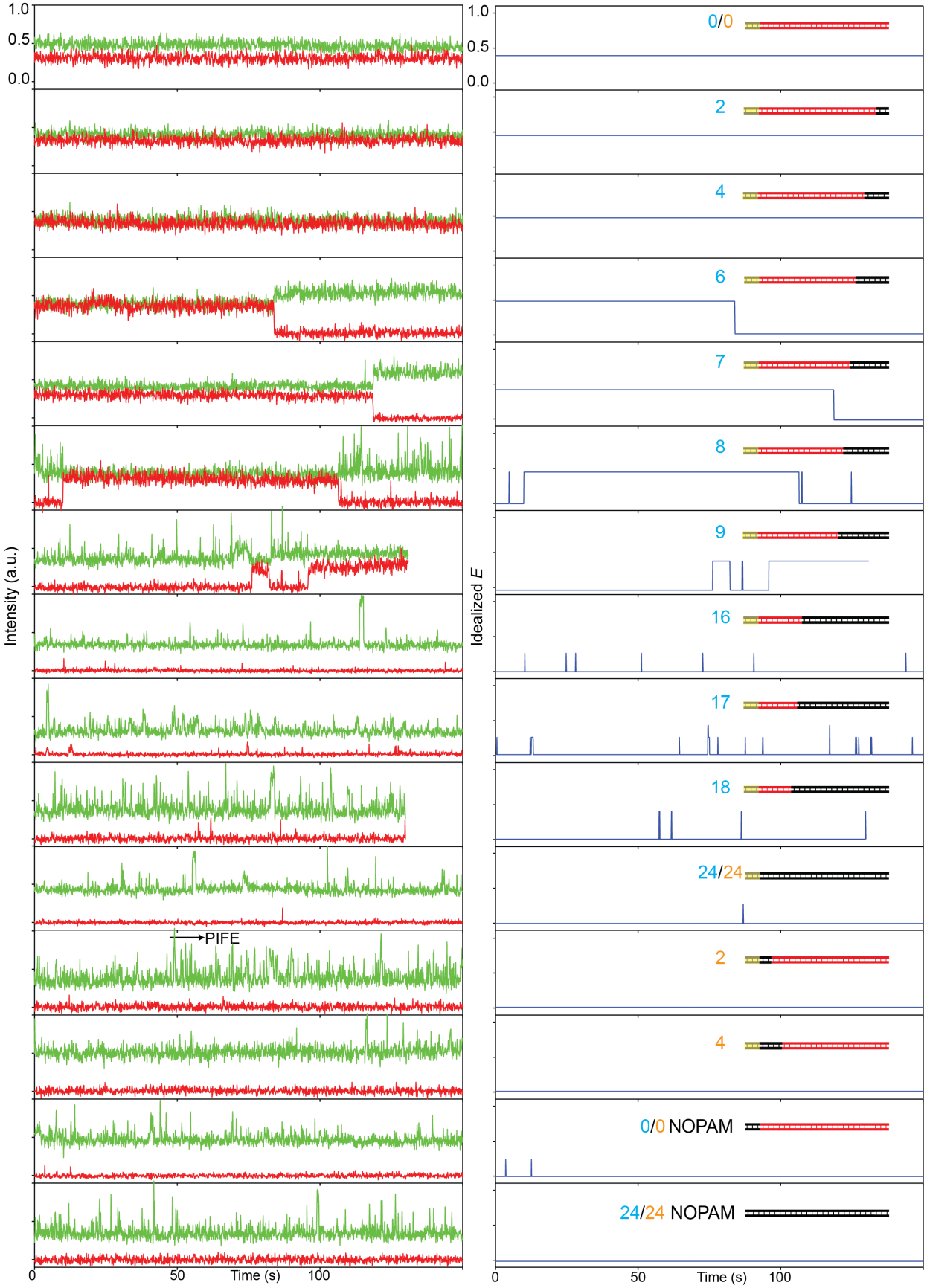
1.0
0.5
0.0
Intensity (a.u.)
PIFE
0
50
Time (s)
100
Idealized E
0/0
2
4
6
7
8
9
16
17
18
24/24
2
4
0/0 NOPAM
24/24 NOPAM

**Figure S7.** Representative smFRET time-trajectories from smFRET experiments to study DNA interrogation by LbCpf1-RNA.

These representative smFRET time- trajectories (left) along with their idealized FRET values (right) are taken from representative DNA targets with/without nick near the PAM (**Fig. S1**) and no differences were observed between them. The indicated protein induced fluorescence enhancement (PIFE) on the donor only signal is likely resulting from non-specific interaction of the free-excess of Apo LbCpf1 with the DNA and was observed for all the DNA targets. DNA targets with nick (**Fig. S1**) exhibit stronger anti-correlation between donor and acceptor signal for transient FRET binding events. PIFE upon the LbCpf1-RNA binding can influence this anti-correlation and slightly different levels of PIFE on Cy3 in DNA target with and without nick i.e. different flexibilities could be causing these variations. Photophysics or isomerization of Cy3 resulting PIFE is guided by local DNA flexibility(5). Number of PAM-distal ($n_{PD}$) and PAM-proximal mismatches ($n_{PP}$) are shown in cyan and orange respectively.

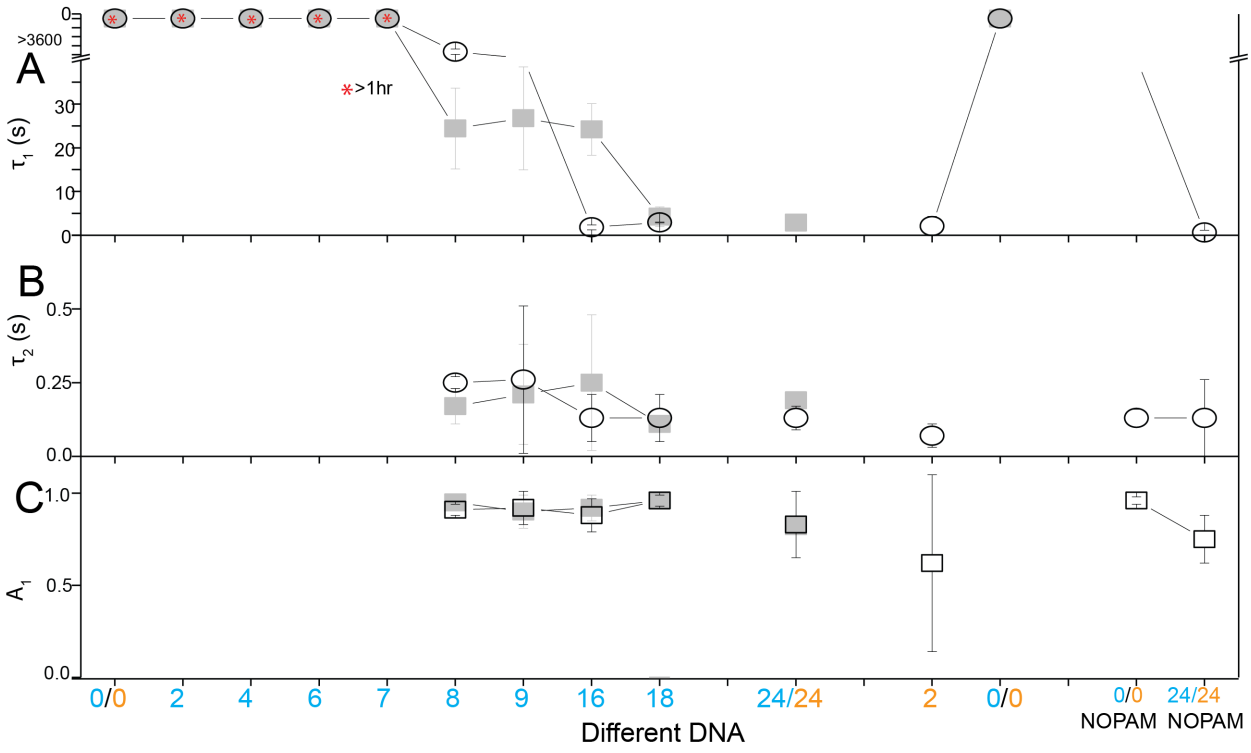


**Figure S8.** Bimodal nature of DNA interrogation by Cpf1-RNA and its parameters.

Survival probability of FRET state ($E > 0.2$; putative bound states) and zero FRET state (E<0.2; unbound states) dwell-times vs. time fit with double-exponential, as shown in **Fig. 3E,** which results in two binding modes (**Fig. 3F**; with their lifetimes $\tau_1$ and $\tau_2$ respectively. The resultant amplitude-weighted lifetime (of $\tau_1$ and $\tau_2$), $\tau_{avg}$, of the Cpf1-RNA bound state is shown in **Fig. 3F**. (*A*) Lifetime of long-lived binding mode ($\tau_1$). (*B*) Lifetime of transient ($\tau_2$) binding mode which was similar for all the DNA targets (~ <0.5 s). (*C*) Amplitude of the transient binding mode only.

Error bars represent s.d. for 2 replicate experiments. Large error bars were observed due to the under-sampling (i.e. below detection limit of 0.1s) of extremely transient binding events for certain DNA targets, especially with PAM-proximal mismatches or without PAM. This indicates that Cpf1-RNA rejected DNA faster if there were PAM-proximal mismatches or in absence of PAM. Number of PAM-distal ($n_{PD}$) and PAM-proximal mismatches ($n_{PP}$) are shown in cyan and orange respectively.

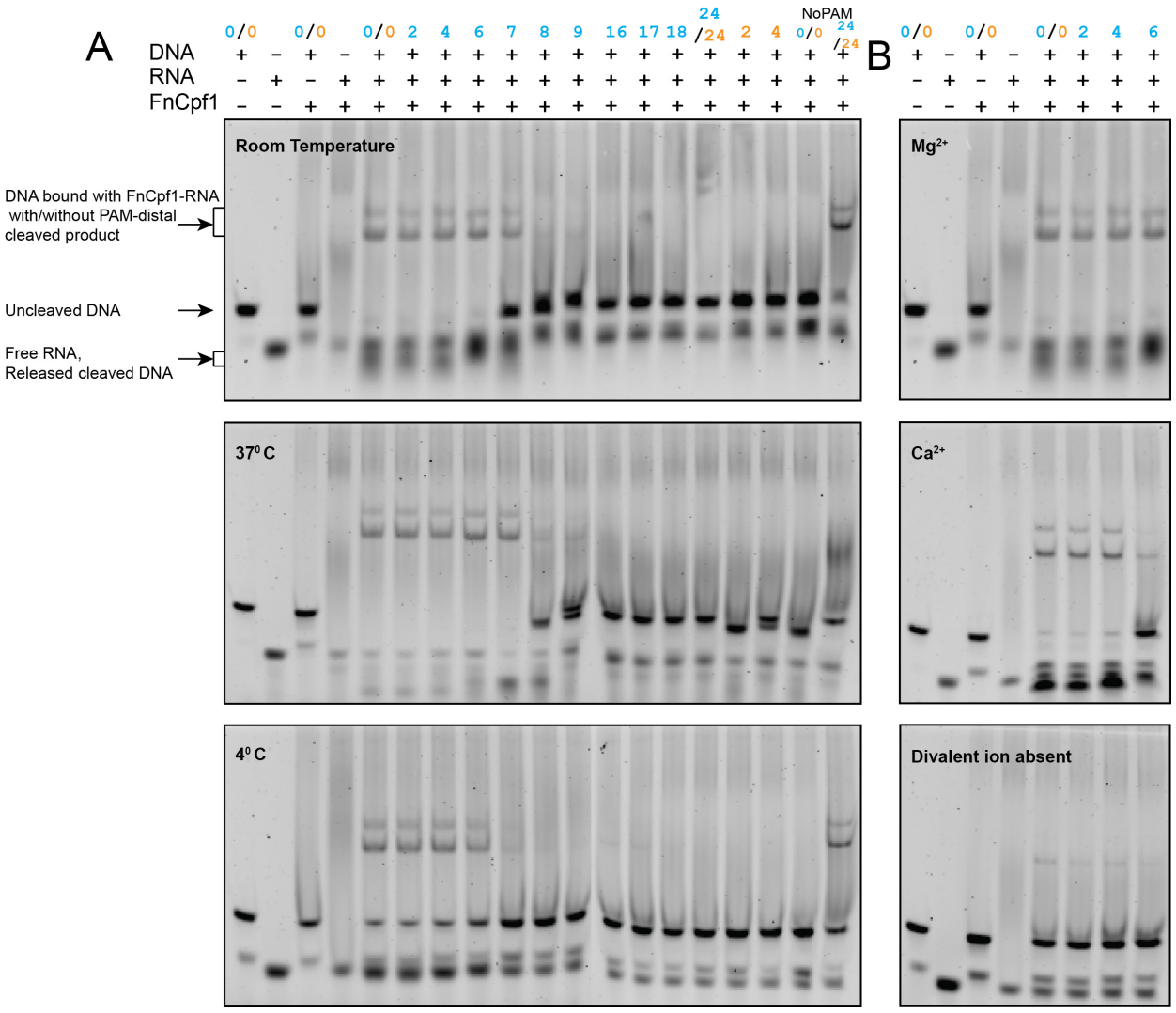


**Figure S9.** FnCpf1 activity at different temperatures and divalent cation conditions.

DNA cleavage and binding by FnCpf1 at (*A*) different temperature and (*B*) divalent cation conditions analyzed by 4% native agarose gel electrophoresis and SYBR Gold II staining of nucleic acids. (*A*) DNA targets with $n_{PD}$ ranging from 0 to 7 were stably bound and cleaved by FnCpf1, as seen from depletion of uncleaved DNA band for these DNA targets. Binding and cleavage cut-off was observed at $n_{PD} = 7$ (substantially reduced cleavage activity), beyond which all the DNA targets remained unbound and uncleaved. FnCpf1 remained active across different temperatures but its efficiency was higher at 37 °C and lower at 4 °C compared to room temperature. Also, differences in cleavage efficiency $n_{PD} = 7$ were markedly different across different temperature conditions. (*B*) Divalent cation is crucial for DNA

targeting and cleavage by FnCpf1 as shown by the fully intact uncleaved DNA target band (bottom) for experiments without divalent cation, the binding was also significantly impaired for such cases with a faint band corresponding to the FnCpf1-RNA-DNA complex. Both $Ca^{2+}$ and $Mg^{2+}$ supported the FnCpf1 binding and cleavage activity (top, middle). All these experiments were performed with short dsDNA targets with only 6 bp flanking the protospacer (4 of which is for PAM). These results also underlie FnCpf1's ability to affect interference on short dsDNA targets. Sequences of DNA targets and guide-RNA used for these experiments is in **Table S3, S5**. Number of PAM-distal ($n_{PD}$) and PAM-proximal mismatches ($n_{PP}$) are shown in cyan and orange respectively.

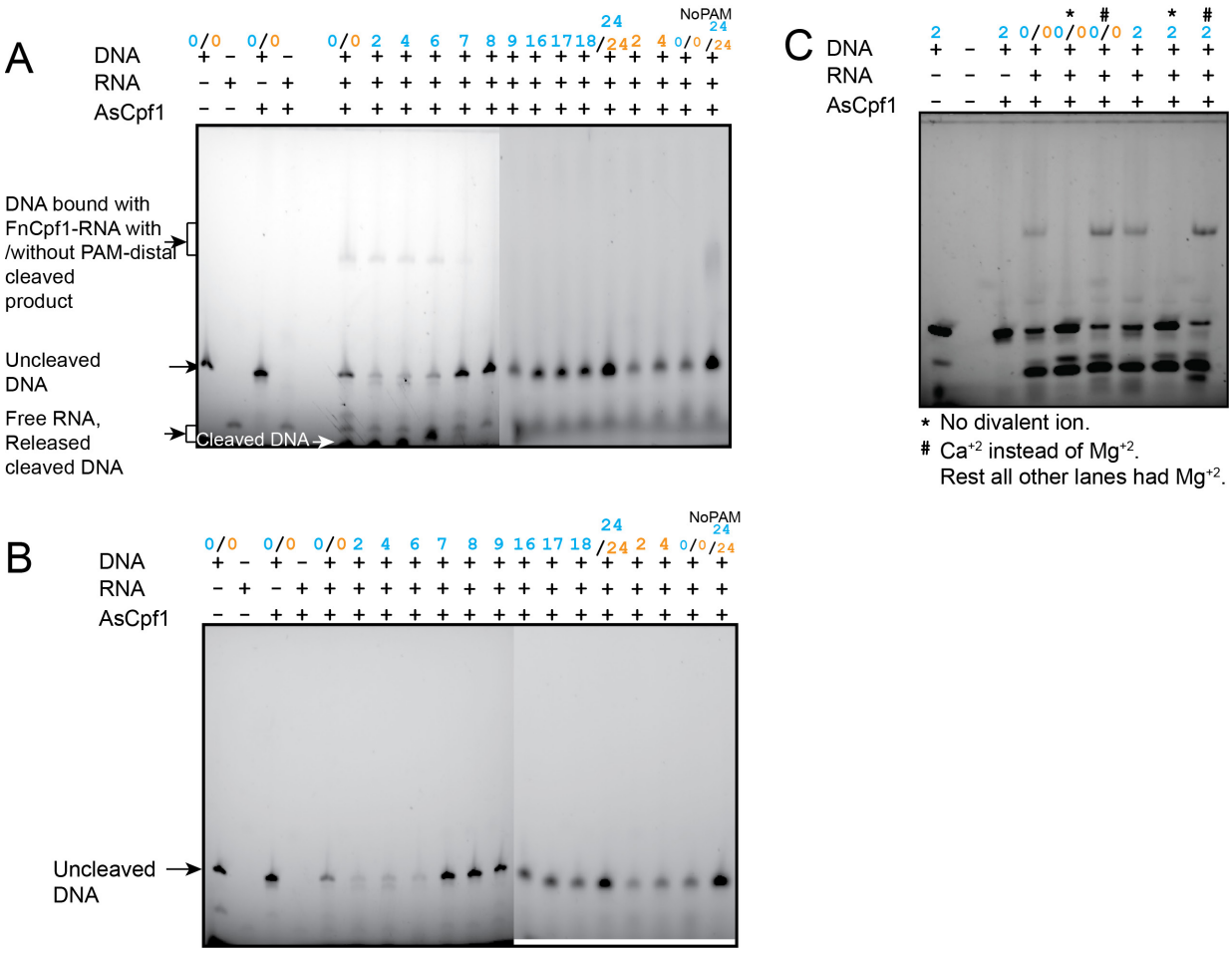


**Figure S10.** AsCpf1-RNA activity and effect of divalent cation conditions.

(*A*) DNA cleavage & binding by AsCpf1 at room temperature analyzed by 4% (*A*) native and (*B*) denaturing agarose gel electrophoresis and SYBR Gold II staining of nucleic acids. (*A-B*) DNA targets with $n_{PD}$ ranging from 0 to 7 were stably bound and cleaved by AsCpf1, as seen from depletion of uncleaved DNA band for these DNA targets. Binding and cleavage cut-off was observed at $n_{PD} = 7$ (substantially reduced cleavage activity), beyond which all the DNA targets remained unbound and uncleaved. (*C*) Divalent cation is crucial for DNA targeting and cleavage by AsCpf1 as shown by the fully intact uncleaved DNA target band (bottom) for experiments without divalent cation, the binding was also significantly impaired for such cases with a faint band corresponding to the AsCpf1-RNA-DNA complex. Both $Ca^{2+}$ and $Mg^{2+}$ supported the AsCpf1 binding and cleavage activity (top, middle). All these

experiments were performed with short dsDNA targets with only 6 bp flanking the protospacer (4 of which is for PAM). These results also underlie AsCpf1's ability to affect interference on short dsDNA targets. Sequences of DNA targets and guide-RNA used for these experiments is in **Table S3, S5**. All these experiments were performed in pH 8.0 conditions, and it was later discovered (**Fig. S4**) that AsCpf1 shows strong pH dependence and works efficiently only at pH 6.5-7.0. Therefore, all subsequent experiments were performed at pH 7.0. Lower activity of the experiments shown here can be attributed to its high pH conditions. Number of PAM-distal ($n_{PD}$) and PAM-proximal mismatches ($n_{PP}$) are shown in cyan and orange respectively.

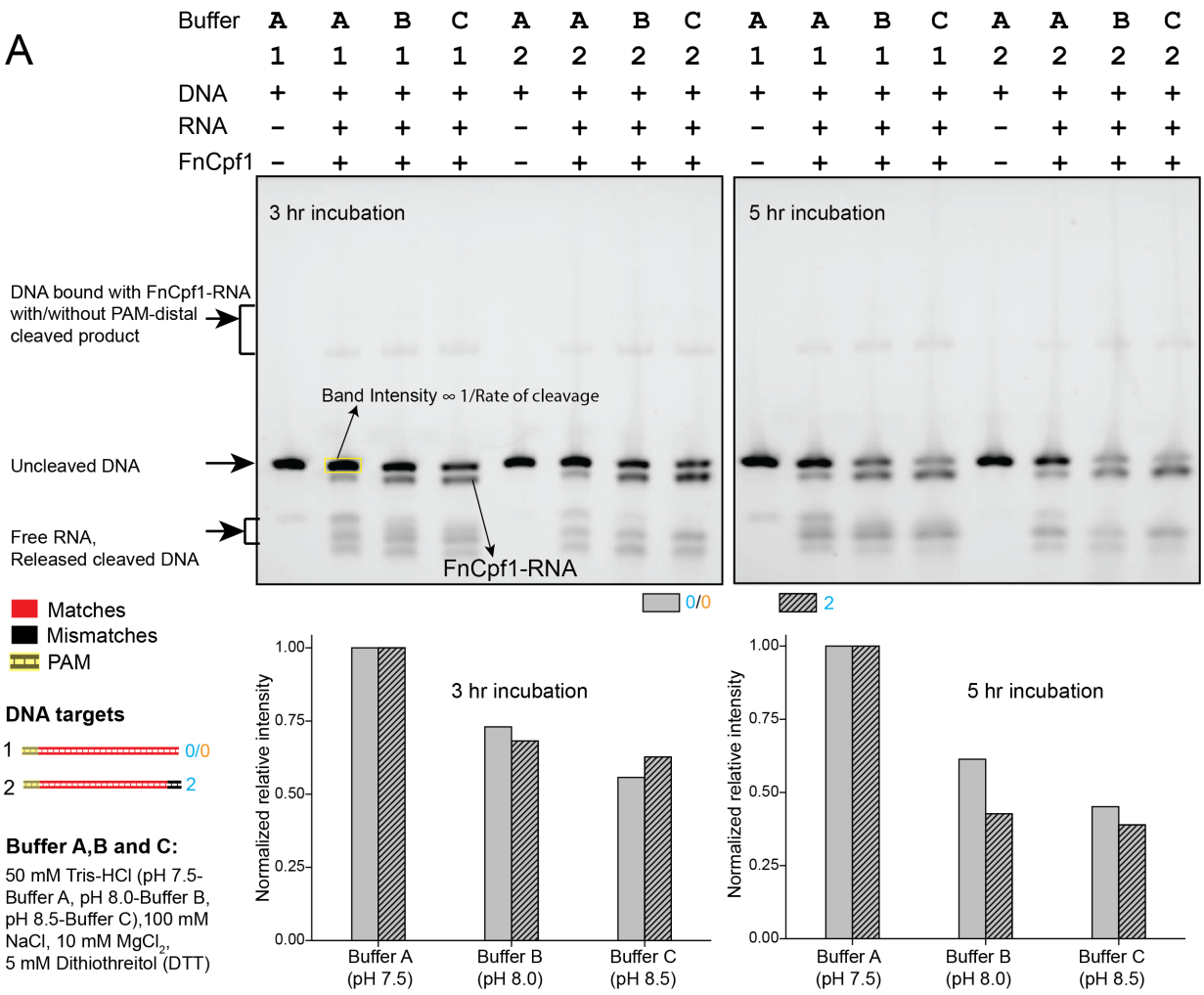


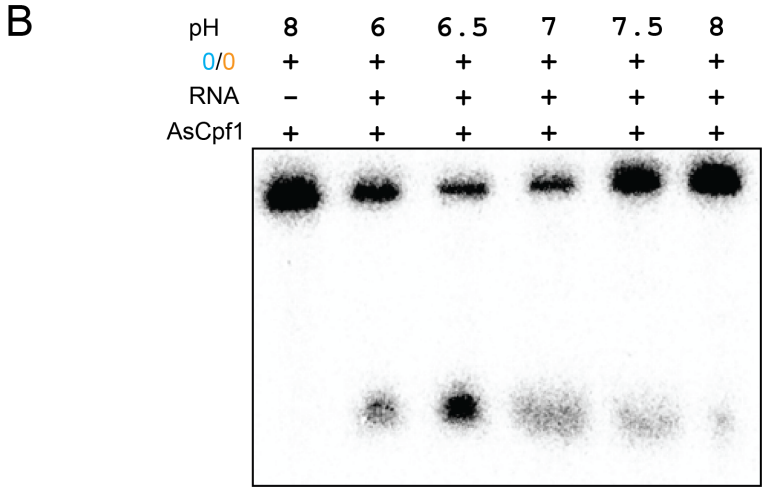


**Figure S11.** Cpf1-RNA activity at different pH conditions.

(*A*) FnCpf1-RNA DNA cleavage and binding reactions incubated for 3 and 5 hr at different pH conditions analyzed by 4% native agarose gel electrophoresis and SYBR Gold II staining of nucleic acids. 60 nM of DNA targets was mixed with the ~300 nM of FnCpf1-RNA in reaction buffer volume of 20 µL. 10 µL of the reaction was analyzed at 3 hr time point and the remaining 10 µL of the reaction was analyzed at 5 hr time point. For the reactions incubated for 3 hr, intensity of the uncleaved DNA target band was taken as being inversely proportional to rate of DNA interference by FnCpf1 and was ~37% and ~79% higher when pH of the Tris-HCl component used in the reaction buffer was 8.0 and 8.5 respectively as compared to 7.5. For the reactions incubated for 5 hr, the rate of cleavage was ~46% and ~59% higher when pH of the Tris-HCl component used in the reaction buffer was 8.0 and 8.5 respectively as compared to 7.5. (*B*) Effect of pH on AsCpf1 activity. Sequences of DNA targets and guide-RNA used for these experiments is in **Table S3** and **S5**. Number of PAM-distal ($n_{PD}$) and PAM-proximal mismatches ($n_{PP}$) are shown in cyan and orange respectively.

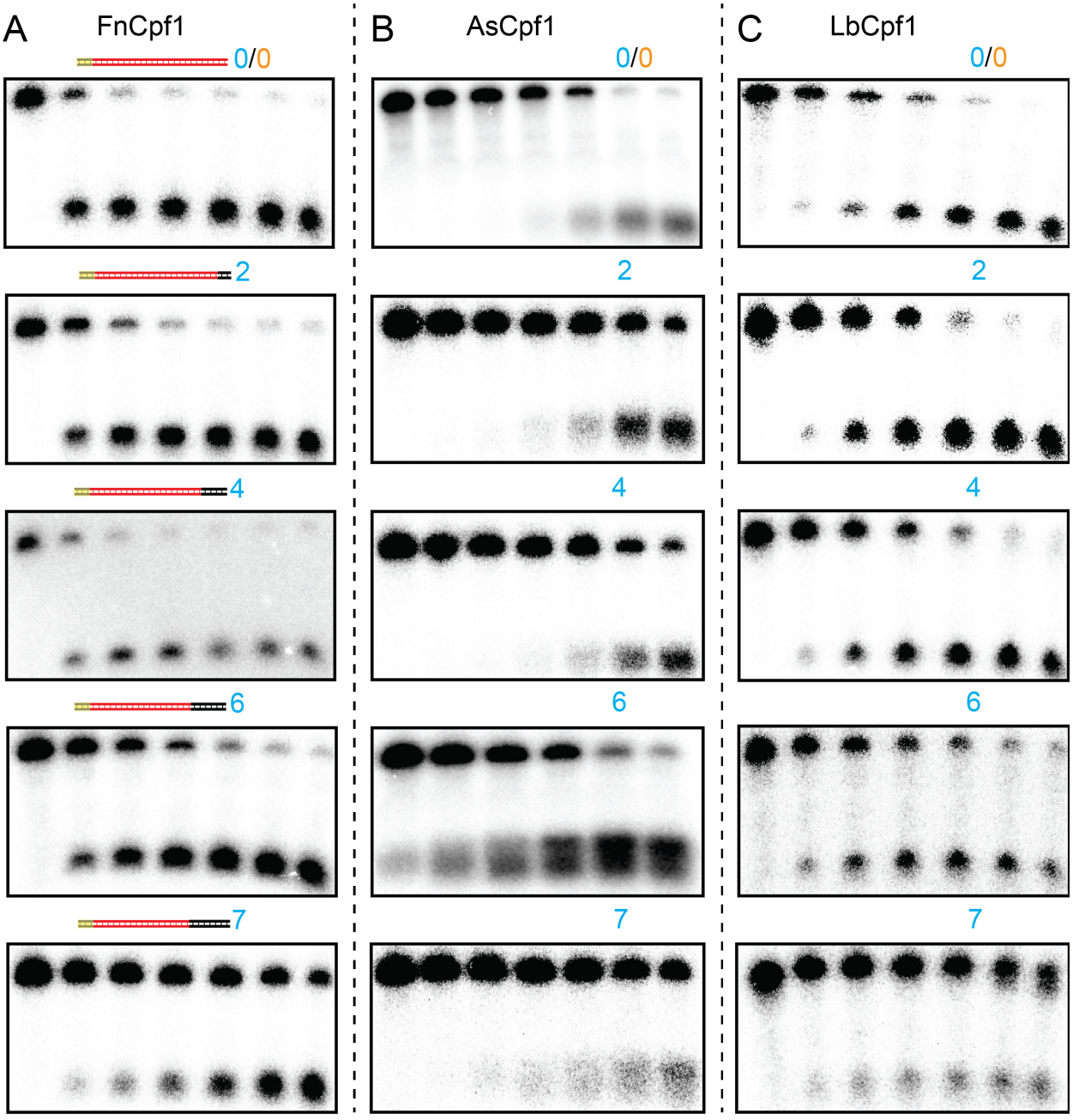


**Figure S12.** Time-lapse of cleavage by Cpf1.

Representative images of cleavage by Cpf1 at room temperature for different DNA targets as a function of time, from experiments utilizing 10% Polyacrylamide denaturing gel electrophoresis. Target strand in DNA targets was radio-labeled. [Cpf1-RNA] =50 nM. [DNA] =0.5 nM. From 3 replicate experiments, uncleaved and cleaved DNA intensities were quantified and their decay fit to single exponential profile

to obtain lifetime of cleavage ($t_{cleavage}$) as shown and quantified in **Fig. 4*B*** and **4*C***. Sequences of DNA targets and guide-RNA used for these experiments is in **Table S2** and **S5**. Number of PAM-distal ($n_{PD}$) and PAM-proximal mismatches ($n_{PP}$) are shown in cyan and orange respectively.

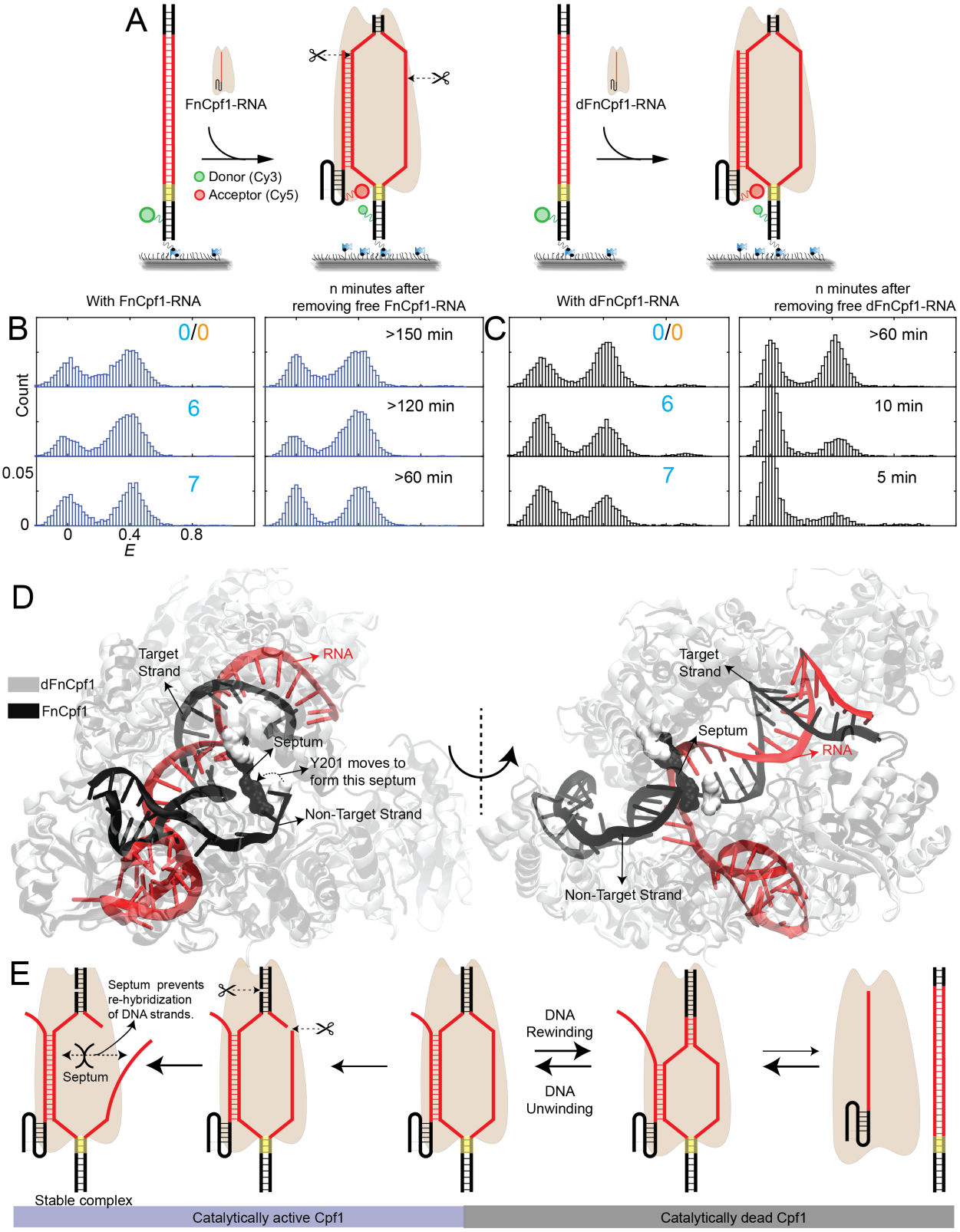


**Figure S13.** Catalytic activity of Cpf1 increases stability of Cpf1-RNA-DNA.

(*A*) Schematic of single-molecule FRET assay to investigate DNA binding by catalytically active FnCpf1 (left) and catalytically dead FnCpf1 (right). DNA cleavage sites are indicated.

(*B*) *E* histograms of different DNA targets with 50 nM FnCpf1-RNA and n minutes post removal of free FnCpf1-RNA from the imaging chamber. (*C*) *E* histograms of different DNA targets with 50 nM dFnCpf1-RNA and n minutes (as indicated) post removal of free FnCpf1-RNA from the imaging chamber. Number of PAM-distal ($n_{PD}$) in DNA targets are shown in cyan. (*D*) The aligned structures of FnCpf1-RNA-DNA (post cleavage) and dFnCpf1-RNA-DNA shows the emergence of a septum separating and preventing the re-hybridization of target and non-target strand emerges after DNA cleavage. (*E*) Internal DNA unwinding and rewinding dynamics in Cpf1-RNA-DNA likely causes eventual disassociation of Cpf1-RNA from DNA. The emergence of septum post DNA cleavage, stalls the unwinding/rewinding dynamics thus preventing Cpf1-RNA dissociation leading to a stable Cpf1-RNA-DNA.

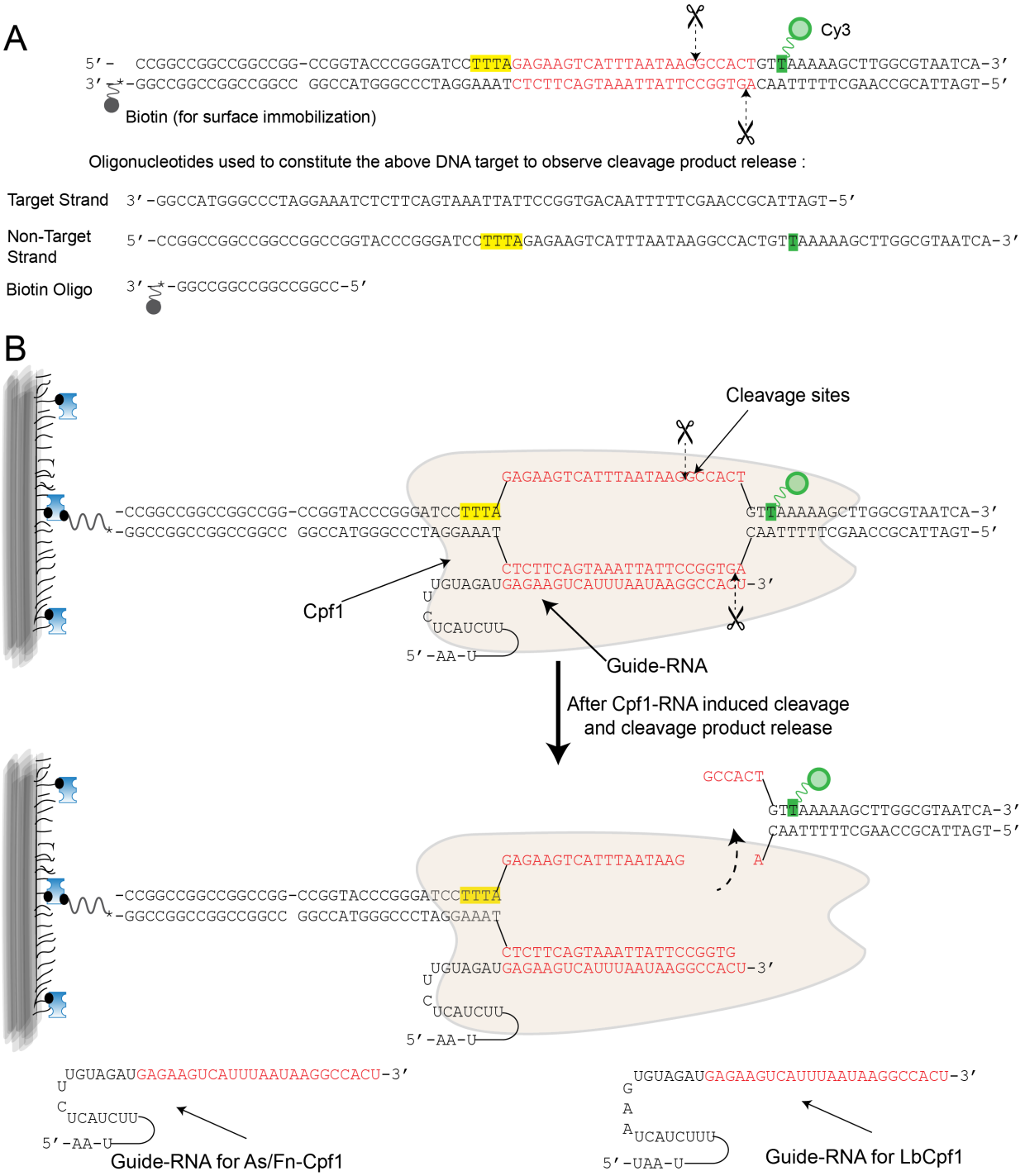


**Figure S14.** Design of DNA targets and guide-RNA for single-molecule cleavage product release assay to study Cpf1-RNA induced cleavage product release of DNA targets.

(*A*) Description of single-stranded DNA oligonucleotides with appropriate modifications for constitution of a fully duplexed DNA target for use in the single-molecule cleavage product release assay. Oligonucleotides referred to as Biotin oligo provide anchor for surface immobilization of the fully duplexed DNA target. These oligonucleotides were same for all the DNA targets. The other two strands being, target strand that hybridizes with the guide-RNA (of Cpf1-RNA) and non-target strand, complementary to the target strand. The non-target strand was labeled with Cy3 at the indicated position. Base sequence of the target and non-target strands were changed to create DNA targets with mismatches against the fixed guide-RNA sequence. (*B*) Illustrated schematic of a complete Cpf1-RNA-DNA complex showing the base-pairing between different components. Sequence written in red denote the cognate sequence of the DNA target and the complementary sequence in the guide-RNA. Also shown are the guide-RNA sequences used for these experiments.

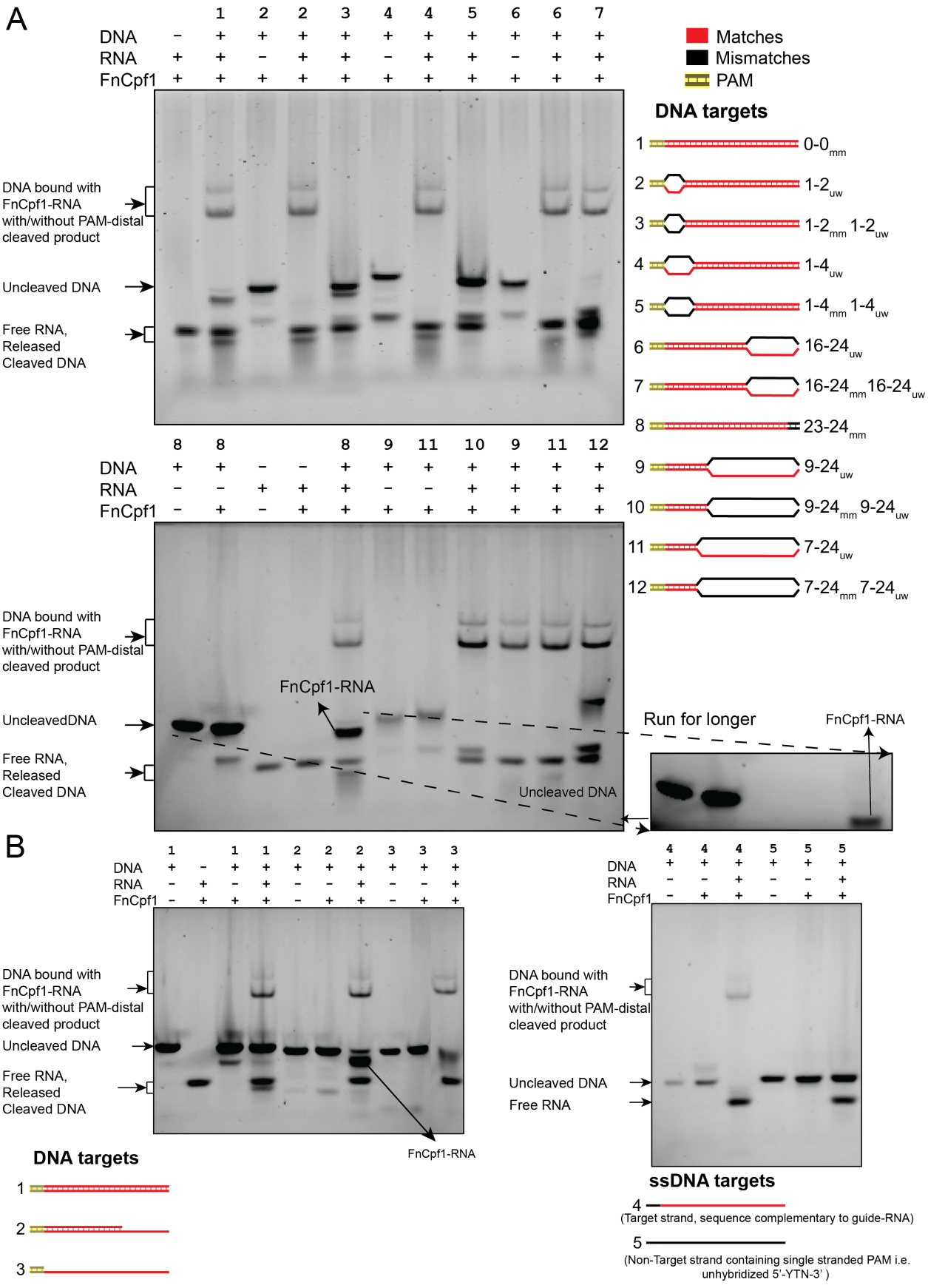
A
Matches
Mismatches
PAM
DNA targets
1 0-0mm
2 1-2uw
3 1-2mm 1-2uw
4 1-4uw
5 1-4mm 1-4uw
6 16-24uw
7 16-24mm 16-24uw
8 23-24mm
9 9-24uw
10 9-24mm 9-24uw
11 7-24uw
12 7-24mm 7-24uw
DNA
RNA
FnCpf1
DNA bound with FnCpf1-RNA with/without PAM-distal cleaved product
Uncleaved DNA
Free RNA, Released Cleaved DNA
UncleavedDNA
FnCpf1-RNA
Run for longer
Uncleaved DNA
B
DNA targets
1
2
3
ssDNA targets
4
(Target strand, sequence complementary to guide-RNA)
5
(Non-Target strand containing single stranded PAM i.e. unhybridized 5'-YTN-3' )
Free RNA

**Figure S15.** FnCpf1 activity for DNA targets in pre-unwound configuration and DNA targets with partially or completely single stranded target strand analyzed by 4% native gel electrophoresis and SYBR Gold II staining of nucleic acids.

(*A*) Pre-unwound DNA targets with mismatches i.e. DNA targets with no base-pairing between target and non-target strands at the indicated bulged portion along with mismatches in the target strand. These were bound and cleaved by FnCpf1-RNA even with high extent of PAM-distal mismatches. This indicates that if DNA unwinding was facilitated by using pre-unwound DNA configuration, then the FnCpf1 was more likely to cause DNA cleavage. But even for pre-unwound DNA targets, PAM-proximal complementarity between guide-RNA and the target strand of the DNA targets was still a necessary condition for the FnCpf1 activity. x-$y_{mm}$ refers to a contiguous mismatch (between target strand and the guide-RNA) running from position x to y relative to PAM, whereas x-$y_{uw}$ refers to a contiguous stretch (relative to PAM) in the DNA target where the bases between the target and the non-target strands are not base-paired. FnCpf1-RNA band was sometimes observed as a faint band right below the uncleaved DNA target band. Possibly, complexation of guide-RNA with FnCpf1 prevents efficient staining of RNA in the FnCpf1-RNA. As shown, if the gel-electrophoresis was run longer, then a clearer resolution between uncleaved DNA target and FnCpf1-RNA band could be observed. (*B*) Partially duplex DNA targets, i.e., DNA targets with a portion of target strand in single-stranded confirmation were also bound and cleaved by FnCpf1 even if the PAM was single-stranded.

Sequences of DNA targets and guide-RNA used for all these experiments is in **Table S3-S5**.

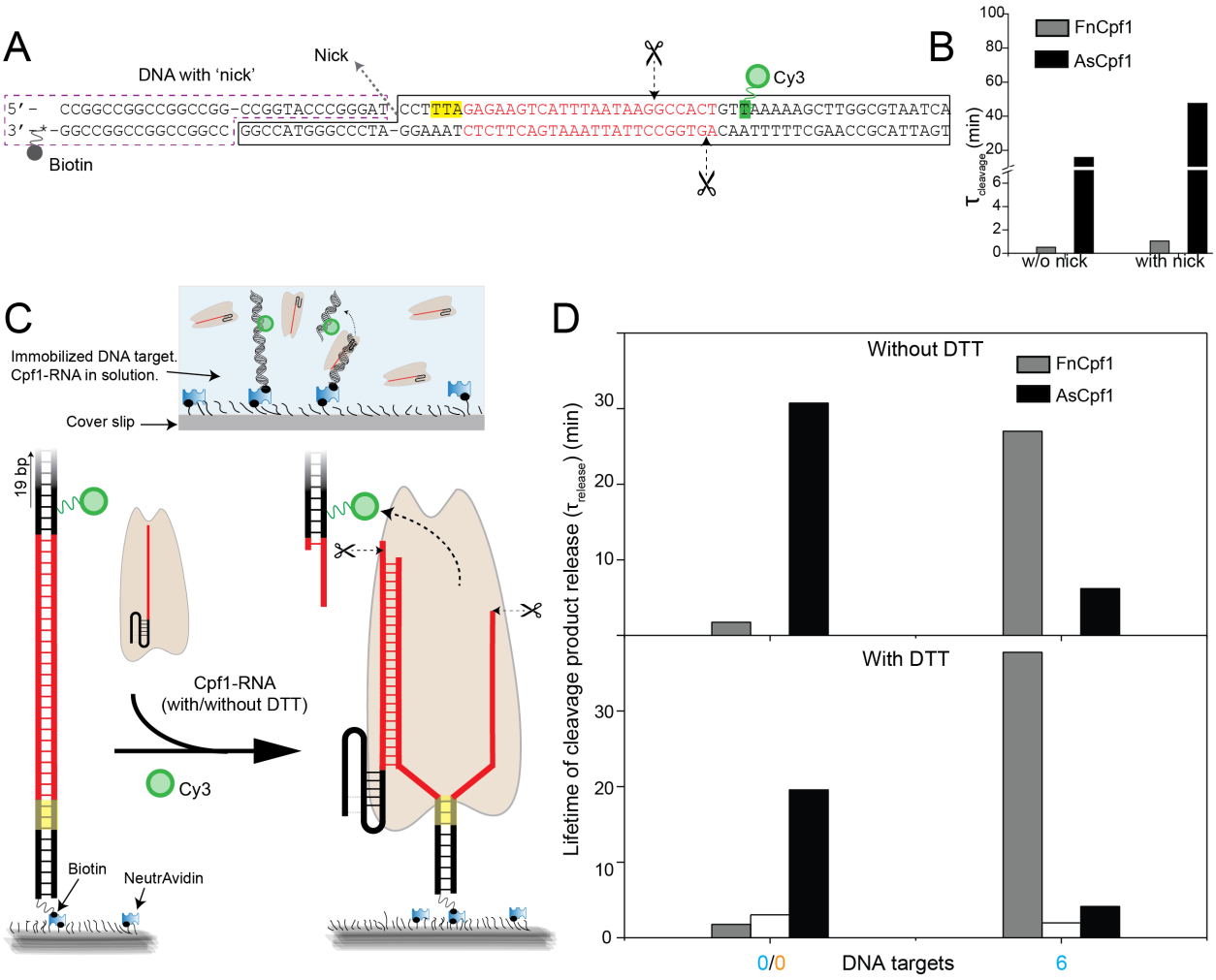


**Figure S16.** Effect of 'nick' and reducing conditions on the Cpf1 induced DNA cleavage and release of cleavage products.

(*A*) Presence of nick close to PAM can perturb DNA bending, which has been structurally characterized(6) to be important for Cas9 induced DNA unwinding or R-Loop formation, which in turn guides cleavage action as per our unpublished study. To probe its effect in cleavage action of Cpf1, the radio-labeled denaturing gel-electrophoresis experiments (**Fig. 4*B***) were performed to measure lifetime of cleavage with and without the nick. Values of which are shown in (*B*). Cleavage is 2-3-fold slower in presence of nick. Here, the values without nick are same as the ones shown in **Fig. 4*C***. (*C*) Schematic of single-molecule cleavage product release assay as described in **Fig. 4*D***. These experiments were done in reducing and non-reducing conditions i.e. with and without DTT. Lifetime of cleavage product release

with and without DTT is summarized in (*D*). Here, the values without nick are the same as the ones shown in **Fig. 4*F*.** FnCpf1 and AsCpf1 activity were similar, as we have shown previously that their activity is not much affected by reducing conditions. But LbCpf1 which we have shown to be strongly dependent on reducing conditions had the most effect in absence of reducing conditions as shown.

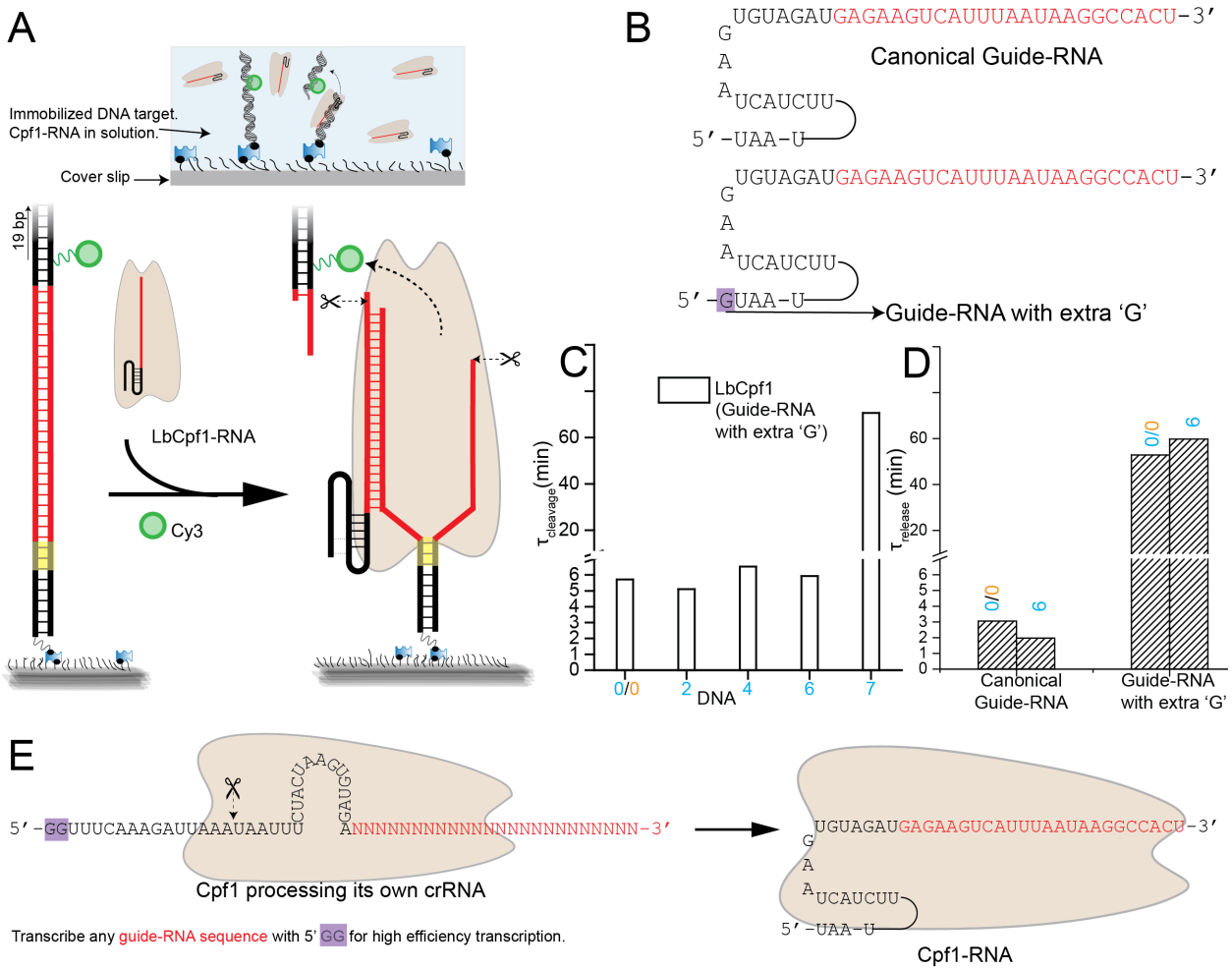


**Figure S17.** Effect of an extra guanine (G) base in guide-RNA for LbCpf1-RNA activity.

(*A*) Schematic of the single-molecule cleavage product release assay as described in **Fig. 4*D*** and **Fig. S14**. (*B*) Two different guide-RNA sequences tested for LbCpf1-RNA. Former is the canonical guide-RNA for LbCpf1 as has been described(7). The latter is the guide-RNA we *in-vitro* transcribed for testing with LbCpf1, which has an extra guanine (G) at the 5’ end. (*C*) $t_{cleavage}$ by LbCpf1 with guide-RNA with the extra G at the 5’ end. (*D*) Extra G is quite deleterious for LbCpf1-RNA activity as shown by many-fold increase in the lifetime of cleavage-product release. (*E*) This problem of 5’ G can be solved by transcribing RNAs with 5’ G containing CRISPR repeat. Cpf1 is the most minimalist CRISPR system as it processes its own guide-RNA (crRNA). The transcribed RNA with 5’ G containing CRISPR repeat will be processed out by Cpf1 itself to produce mature guide-RNAs(8) as shown in the schematic.

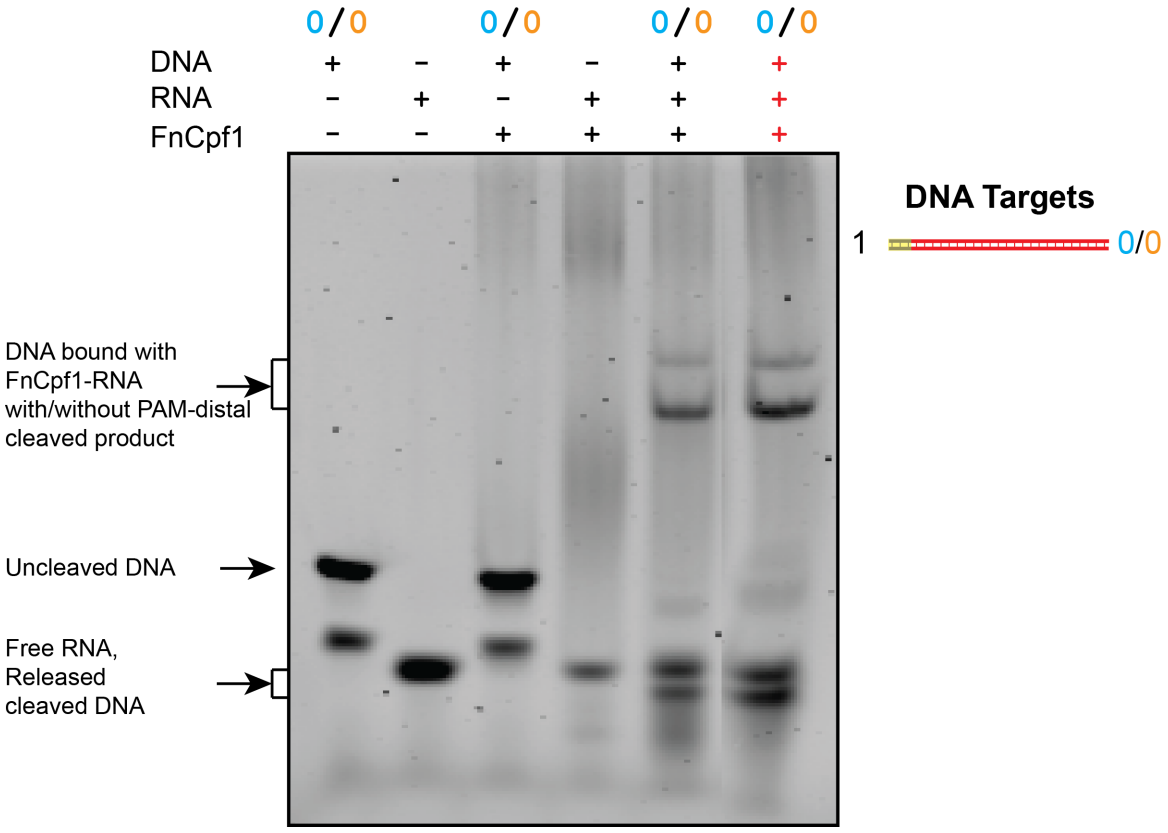


**Figure S18.** FnCpf1 activity is not affected by the imaging buffer components.

DNA cleavage & binding by FnCpf1 analyzed by 4% native gel electrophoresis and SYBR Gold II staining of nucleic acids. Lanes colored with black legends used the reaction buffer (50 mM Tris-HCl (pH 8.0), 100 mM NaCl, 10 mM $MgCl_2$, 5 mM Dithiothreitol (DTT)) while the lane colored with red legend used reaction buffer containing Trolox and BSA i.e. imaging buffer components (50 mM Tris-HCl (pH 8.0), 100 mM NaCl, 10 mM $MgCl_2$, 5 mM Dithiothreitol (DTT), 0.2 mg/ml BSA and saturated Trolox (>5 mM). Sequences of DNA targets and guide-RNA used for these experiments is in **Table S3** and **S5**.

**Table S1. List of DNA targets used in smFRET experiments to study DNA interrogation by Cpf1-RNA.**

| Description | DNA Sequences |
|---|---|
| 0/0 | 16 nucleotide biotinylated adaptor for surface immobilization<br>5′- CAGTCCTGCTGGTCGT-TCGGTACCCGGGATCCTTTAGAGAAGTCATTTAATAAGGCCACTGTTAAAAAGCTTGGCGTAATCA- 3′<br>3′-*-GTCAGGACGACCAGCA AGCCATGGGCCCTAGGAAATCTCTTCAGTAAATTATTCCGGTGACAATTTTTCGAACCGCATTAGT- 5′ |
| 2 | 5′- CAGTCCTGCTGGTCGT-TCGGTACCCGGGATCCTTTAGAGAAGTCATTTAATAAGGCCAGAGTTAAAAAGCTTGGCGTAATCA- 3′<br>3′-*-GTCAGGACGACCAGCA AGCCATGGGCCCTAGGAAATCTCTTCAGTAAATTATTCCGGTCTCAATTTTTCGAACCGCATTAGT- 5′ |
| 4 | 5′- CAGTCCTGCTGGTCGT-TCGGTACCCGGGATCCTTTAGAGAAGTCATTTAATAAGGCGTGAGTTAAAAAGCTTGGCGTAATCA- 3′<br>3′-*-GTCAGGACGACCAGCA AGCCATGGGCCCTAGGAAATCTCTTCAGTAAATTATTCCGCACTCAATTTTTCGAACCGCATTAGT- 5′ |
| 6 | 5′- CAGTCCTGCTGGTCGT-TCGGTACCCGGGATCCTTTAGAGAAGTCATTTAATAAGCGGTGAGTTAAAAAGCTTGGCGTAATCA- 3′<br>3′-*-GTCAGGACGACCAGCA AGCCATGGGCCCTAGGAAATCTCTTCAGTAAATTATTCGCCACTCAATTTTTCGAACCGCATTAGT- 5′ |
| 7 | 5′- CAGTCCTGCTGGTCGT-TCGGTACCCGGGATCCTTTAGAGAAGTCATTTAATAACCGGTGAGTTAAAAAGCTTGGCGTAATCA- 3′<br>3′-*-GTCAGGACGACCAGCA AGCCATGGGCCCTAGGAAATCTCTTCAGTAAATTATTGGCCACTCAATTTTTCGAACCGCATTAGT- 5′ |
| 8 | 5′- CAGTCCTGCTGGTCGT-TCGGTACCCGGGATCCTTTAGAGAAGTCATTTAATATCCGGTGAGTTAAAAAGCTTGGCGTAATCA- 3′<br>3′-*-GTCAGGACGACCAGCA AGCCATGGGCCCTAGGAAATCTCTTCAGTAAATTATAGGCCACTCAATTTTTCGAACCGCATTAGT- 5′ |
| 9 | 5′- CAGTCCTGCTGGTCGT-TCGGTACCCGGGATCCTTTAGAGAAGTCATTTAATTTCCGGTGAGTTAAAAAGCTTGGCGTAATCA- 3′<br>3′-*-GTCAGGACGACCAGCA AGCCATGGGCCCTAGGAAATCTCTTCAGTAAATTAAAGGCCACTCAATTTTTCGAACCGCATTAGT- 5′ |
| 16 | 5′- CAGTCCTGCTGGTCGT-TCGGTACCCGGGATCCTTTAGAGAAGTCTAAATTATTCCGGTGAGTTAAAAAGCTTGGCGTAATCA- 3′<br>3′-*-GTCAGGACGACCAGCA AGCCATGGGCCCTAGGAAATCTCTTCAGATTTAATAAGGCCACTCAATTTTTCGAACCGCATTAGT- 5′ |
| 17 | 5′- CAGTCCTGCTGGTCGT-TCGGTACCCGGGATCCTTTAGAGAAGTGTAAATTATTCCGGTGAGTTAAAAAGCTTGGCGTAATCA- 3′<br>3′-*-GTCAGGACGACCAGCA AGCCATGGGCCCTAGGAAATCTCTTCACATTTAATAAGGCCACTCAATTTTTCGAACCGCATTAGT- 5′ |
| 18 | 5′- CAGTCCTGCTGGTCGT-TCGGTACCCGGGATCCTTTAGAGAAGAGTAAATTATTCCGGTGAGTTAAAAAGCTTGGCGTAATCA- 3′<br>3′-*-GTCAGGACGACCAGCA AGCCATGGGCCCTAGGAAATCTCTTCTCATTTAATAAGGCCACTCAATTTTTCGAACCGCATTAGT- 5′ |
| 24/24 | 5′- CAGTCCTGCTGGTCGT-TCGGTACCCGGGATCCTTTACTCTTCAGTAAATTATTCCGGTGAGTTAAAAAGCTTGGCGTAATCA- 3′<br>3′-*-GTCAGGACGACCAGCA AGCCATGGGCCCTAGGAAATGAGAAGTCATTTAATAAGGCCACTCAATTTTTCGAACCGCATTAGT- 5′ |
| 2 | 5′- CAGTCCTGCTGGTCGT-TCGGTACCCGGGATCCTTTACTGAAGTCATTTAATAAGGCCACTGTTAAAAAGCTTGGCGTAATCA- 3′<br>3′-*-GTCAGGACGACCAGCA AGCCATGGGCCCTAGGAAATGACTTCAGTAAATTATTCCGGTGACAATTTTTCGAACCGCATTAGT- 5′ |
| 4 | 5′- CAGTCCTGCTGGTCGT-TCGGTACCCGGGATCCTTTACTCTAGTCATTTAATAAGGCCACTGTTAAAAAGCTTGGCGTAATCA- 3′<br>3′-*-GTCAGGACGACCAGCA AGCCATGGGCCCTAGGAAATGAGATCAGTAAATTATTCCGGTGACAATTTTTCGAACCGCATTAGT- 5′ |
| 0/0 NOPAM | 5′- CAGTCCTGCTGGTCGT-TCGGTACCCGGGATCCACGGGAGAAGTCATTTAATAAGGCCACTGTTAAAAAGCTTGGCGTAATCA- 3′<br>3′-*-GTCAGGACGACCAGCA AGCCATGGGCCCTAGGTGCCCTCTTCAGTAAATTATTCCGGTGACAATTTTTCGAACCGCATTAGT- 5′ |
| 24/24 NOPAM | 5′- CAGTCCTGCTGGTCGT-TCGGTACCCGGGATCCAGGCCTCTTCAGTAAATTATTCCGGTGAGTTAAAAAGCTTGGCGTAATCA- 3′<br>3′-*-GTCAGGACGACCAGCA AGCCATGGGCCCTAGGTCCGGAGAAGTCATTTAATAAGGCCACTCAATTTTTCGAACCGCATTAGT- 5′ |

Thymine modification for Cy3 labeling. *Biotin. PAM. DNA sequences complementary to guide RNA are shown in red (Cognate). Originally DNA targets were created with a 'nick' at AT-CCA near PAM. The nick did not affect binding and 2 replicates of smFRET experiments to study DNA interrogation by Cpf1-RNA was done without nick and one with nick respectively.

**Table S2. List of DNA targets used in all radio-labeled gel electrophoresis experiments**

| Description | DNA Sequences |
|---|---|
| 0/0 | 32P-5′-CAGTCCTGCTGGTCGT-TCGGTACCCGGGATCCTTTAGAGAAGTCATTTAATAAGGCCACTGTTAAAAAGCTTGGCGTAATCA-3′<br>AGCCATGGGCCCTAGGAAATCTCTTCAGTAAATTATTCCGGTGACAATTTTTCGAACCGCATTAGT-5′ |
| 2 | 32P-5′-CAGTCCTGCTGGTCGT-TCGGTACCCGGGATCCTTTAGAGAAGTCATTTAATAAGGCCAGAGTTAAAAAGCTTGGCGTAATCA- 3′<br>AGCCATGGGCCCTAGGAAATCTCTTCAGTAAATTATTCCGGTCTCAATTTTTCGAACCGCATTAGT- 5′ |
| 4 | 32P-5′-CAGTCCTGCTGGTCGT-TCGGTACCCGGGATCCTTTAGAGAAGTCATTTAATAAGGCGTGAGTTAAAAAGCTTGGCGTAATCA- 3′<br>AGCCATGGGCCCTAGGAAATCTCTTCAGTAAATTATTCCGCACTCAATTTTTCGAACCGCATTAGT- 5′ |
| 6 | 32P-5′-CAGTCCTGCTGGTCGT-TCGGTACCCGGGATCCTTTAGAGAAGTCATTTAATAAGCGGTGAGTTAAAAAGCTTGGCGTAATCA- 3′<br>AGCCATGGGCCCTAGGAAATCTCTTCAGTAAATTATTCGCCACTCAATTTTTCGAACCGCATTAGT- 5′ |
| 7 | 32P-5′-CAGTCCTGCTGGTCGT-TCGGTACCCGGGATCCTTTAGAGAAGTCATTTAATAACCGGTGAGTTAAAAAGCTTGGCGTAATCA- 3′<br>AGCCATGGGCCCTAGGAAATCTCTTCAGTAAATTATTGGCCACTCAATTTTTCGAACCGCATTAGT- 5′ |
| 8 | 32P-5′-CAGTCCTGCTGGTCGT-TCGGTACCCGGGATCCTTTAGAGAAGTCATTTAATATCCGGTGAGTTAAAAAGCTTGGCGTAATCA- 3′<br>AGCCATGGGCCCTAGGAAATCTCTTCAGTAAATTATAGGCCACTCAATTTTTCGAACCGCATTAGT- 5′ |
| 9 | 32P-5′-CAGTCCTGCTGGTCGT-TCGGTACCCGGGATCCTTTAGAGAAGTCATTTAATTTCCGGTGAGTTAAAAAGCTTGGCGTAATCA- 3′<br>AGCCATGGGCCCTAGGAAATCTCTTCAGTAAATTAAAGGCCACTCAATTTTTCGAACCGCATTAGT- 5′ |
| 16 | 32P-5′-CAGTCCTGCTGGTCGT-TCGGTACCCGGGATCCTTTAGAGAAGTCTAAATTATTCCGGTGAGTTAAAAAGCTTGGCGTAATCA- 3′<br>AGCCATGGGCCCTAGGAAATCTCTTCAGATTTAATAAGGCCACTCAATTTTTCGAACCGCATTAGT- 5′ |
| 17 | 32P-5′-CAGTCCTGCTGGTCGT-TCGGTACCCGGGATCCTTTAGAGAAGTGTAAATTATTCCGGTGAGTTAAAAAGCTTGGCGTAATCA- 3′<br>AGCCATGGGCCCTAGGAAATCTCTTCACATTTAATAAGGCCACTCAATTTTTCGAACCGCATTAGT- 5′ |
| 18 | 32P-5′-CAGTCCTGCTGGTCGT-TCGGTACCCGGGATCCTTTAGAGAAGAGTAAATTATTCCGGTGAGTTAAAAAGCTTGGCGTAATCA- 3′<br>AGCCATGGGCCCTAGGAAATCTCTTCTCATTTAATAAGGCCACTCAATTTTTCGAACCGCATTAGT- 5′ |
| 24/24 | 32P-5′-CAGTCCTGCTGGTCGT-TCGGTACCCGGGATCCTTTACTCTTCAGTAAATTATTCCGGTGAGTTAAAAAGCTTGGCGTAATCA- 3′<br>AGCCATGGGCCCTAGGAAATGAGAAGTCATTTAATAAGGCCACTCAATTTTTCGAACCGCATTAGT- 5′ |
| 2 | 32P-5′-CAGTCCTGCTGGTCGT-TCGGTACCCGGGATCCTTTACTGAAGTCATTTAATAAGGCCACTGTTAAAAAGCTTGGCGTAATCA- 3′<br>AGCCATGGGCCCTAGGAAATGACTTCAGTAAATTATTCCGGTGACAATTTTTCGAACCGCATTAGT- 5′ |
| 4 | 32P-5′-CAGTCCTGCTGGTCGT-TCGGTACCCGGGATCCTTTACTCTAGTCATTTAATAAGGCCACTGTTAAAAAGCTTGGCGTAATCA- 3′<br>AGCCATGGGCCCTAGGAAATGAGATCAGTAAATTATTCCGGTGACAATTTTTCGAACCGCATTAGT- 5′ |
| 0/0 NOPAM | 32P-5′-CAGTCCTGCTGGTCGT-TCGGTACCCGGGATCCACGGGAGAAGTCATTTAATAAGGCCACTGTTAAAAAGCTTGGCGTAATCA- 3′<br>AGCCATGGGCCCTAGGTGCCCTCTTCAGTAAATTATTCCGGTGACAATTTTTCGAACCGCATTAGT- 5′ |
| 24/24 NOPAM | 32P-5′-CAGTCCTGCTGGTCGT-TCGGTACCCGGGATCCAGGCCTCTTCAGTAAATTATTCCGGTGAGTTAAAAAGCTTGGCGTAATCA- 3′<br>AGCCATGGGCCCTAGGTCCGGAGAAGTCATTTAATAAGGCCACTCAATTTTTCGAACCGCATTAGT- 5′ |

Thymine modification for Cy3 labeling. *Biotin. PAM. DNA sequences complementary to guide RNA are shown in red (Cognate). 32P Radio-label.

**Table S3. List of DNA targets used in gel electrophoresis experiments involving use of SYBR Gold II for staining and visualization of nucleic acid bands.**

| Description | DNA Sequences |
|---|---|
| 0/0 | 5′-CCTTTAGAGAAGTCATTTAATAAGGCCACTGTTAAAAAGCTTGGCGTAATCA- 3′<br>3′-AGCCATGGGCCCTAGGAAATCTCTTCAGTAAATTATTCCGGTGACAATTTTTCGAACCGCATTAGT- 5′ |
| 2 | 5′-CCTTTAGAGAAGTCATTTAATAAGGCCAGAGTTAAAAAGCTTGGCGTAATCA- 3′<br>3′-AGCCATGGGCCCTAGGAAATCTCTTCAGTAAATTATTCCGGTCTCAATTTTTCGAACCGCATTAGT- 5′ |
| 4 | 5′-CCTTTAGAGAAGTCATTTAATAAGGCGTGAGTTAAAAAGCTTGGCGTAATCA- 3′<br>3′-AGCCATGGGCCCTAGGAAATCTCTTCAGTAAATTATTCCGCACTCAATTTTTCGAACCGCATTAGT- 5′ |
| 6 | 5′-CCTTTAGAGAAGTCATTTAATAAGCGGTGAGTTAAAAAGCTTGGCGTAATCA- 3′<br>3′-AGCCATGGGCCCTAGGAAATCTCTTCAGTAAATTATTCGCCACTCAATTTTTCGAACCGCATTAGT- 5′ |
| 7 | 5′-CCTTTAGAGAAGTCATTTAATAACCGGTGAGTTAAAAAGCTTGGCGTAATCA- 3′<br>3′-AGCCATGGGCCCTAGGAAATCTCTTCAGTAAATTATTGGCCACTCAATTTTTCGAACCGCATTAGT- 5′ |
| 8 | 5′-CCTTTAGAGAAGTCATTTAATATCCGGTGAGTTAAAAAGCTTGGCGTAATCA- 3′<br>3′-AGCCATGGGCCCTAGGAAATCTCTTCAGTAAATTATAGGCCACTCAATTTTTCGAACCGCATTAGT- 5′ |
| 9 | 5′-CCTTTAGAGAAGTCATTTAATTTCCGGTGAGTTAAAAAGCTTGGCGTAATCA- 3′<br>3′-AGCCATGGGCCCTAGGAAATCTCTTCAGTAAATTAAAGGCCACTCAATTTTTCGAACCGCATTAGT- 5′ |
| 16 | 5′-CCTTTAGAGAAGTCTAAATTATTCCGGTGAGTTAAAAAGCTTGGCGTAATCA- 3′<br>3′-AGCCATGGGCCCTAGGAAATCTCTTCAGATTTAATAAGGCCACTCAATTTTTCGAACCGCATTAGT- 5′ |
| 17 | 5′-CCTTTAGAGAAGTGTAAATTATTCCGGTGAGTTAAAAAGCTTGGCGTAATCA- 3′<br>3′-AGCCATGGGCCCTAGGAAATCTCTTCACATTTAATAAGGCCACTCAATTTTTCGAACCGCATTAGT- 5′ |
| 18 | 5′-CCTTTAGAGAAGAGTAAATTATTCCGGTGAGTTAAAAAGCTTGGCGTAATCA- 3′<br>3′-AGCCATGGGCCCTAGGAAATCTCTTCTCATTTAATAAGGCCACTCAATTTTTCGAACCGCATTAGT- 5′ |
| 24/24 | 5′-CCTTTACTCTTCAGTAAATTATTCCGGTGAGTTAAAAAGCTTGGCGTAATCA- 3′<br>3′-AGCCATGGGCCCTAGGAAATGAGAAGTCATTTAATAAGGCCACTCAATTTTTCGAACCGCATTAGT- 5′ |
| 2 | 5′-CCTTTACTGAAGTCATTTAATAAGGCCACTGTTAAAAAGCTTGGCGTAATCA- 3<br>3′-AGCCATGGGCCCTAGGAAATGACTTCAGTAAATTATTCCGGTGACAATTTTTCGAACCGCATTAGT- 5′ |
| 4 | 5′-CCTTTACTCTAGTCATTTAATAAGGCCACTGTTAAAAAGCTTGGCGTAATCA- 3′<br>3′-AGCCATGGGCCCTAGGAAATGAGATCAGTAAATTATTCCGGTGACAATTTTTCGAACCGCATTAGT- 5′ |
| 0/0 NOPAM | 5′-CCACGGGAGAAGTCATTTAATAAGGCCACTGTTAAAAAGCTTGGCGTAATCA- 3′<br>3′-AGCCATGGGCCCTAGGTGCCCTCTTCAGTAAATTATTCCGGTGACAATTTTTCGAACCGCATTAGT- 5′ |
| 24/24 NOPAM | 5′-CCAGGCCTCTTCAGTAAATTATTCCGGTGAGTTAAAAAGCTTGGCGTAATCA- 3′<br>3′-AGCCATGGGCCCTAGGTCCGGAGAAGTCATTTAATAAGGCCACTCAATTTTTCGAACCGCATTAGT- 5′ |

PAM. DNA sequences complementary to guide RNA are shown in red (Cognate).

**Table S4. Pre-unwound DNA targets used in gel electrophoresis experiments involving use of SYBR Gold II for staining and visualization of nucleic acid bands.**

| Description | DNA Sequences |
|---|---|
| 1-2mm 1-2uw | 5′-CCTTTAGAGAAGTCATTTAATAAGGCCACTGTTAAAAAGCTTGGCGTAATCA- 3′<br>3′-AGCCATGGGCCCTAGGAAATGACTTCAGTAAATTATTCCGGTGACAATTTTTCGAACCGCATTAGT- 5′ |
| 1-2uw | 5′-CCTTTAGAGAAGTCATTTAATAAGGCCACTGTTAAAAAGCTTGGCGTAATCA- 3′<br>3′-AGCCATGGGCCCTAGGAAATGACTTCAGTAAATTATTCCGGTGACAATTTTTCGAACCGCATTAGT- 5′ |
| 1-4mm 1-4uw | 5′-CCTTTAGAGAAGTCATTTAATAAGGCCACTGTTAAAAAGCTTGGCGTAATCA- 3′<br>3′-AGCCATGGGCCCTAGGAAATGAGATCAGTAAATTATTCCGGTGACAATTTTTCGAACCGCATTAGT- 5′ |
| 1-4uw | 5′-CCTTTACTCTAGTCATTTAATAAGGCCACTGTTAAAAAGCTTGGCGTAATCA- 3′<br>3′-AGCCATGGGCCCTAGGAAATCTCTTCAGTAAATTATTCCGGTGACAATTTTTCGAACCGCATTAGT- 5′ |
| 16-24mm 16-24uw | 5′-CCTTTAGAGAAGTCATTTAATTTCCGGTGAGTTAAAAAGCTTGGCGTAATCA- 3′<br>3′-AGCCATGGGCCCTAGGAAATCTCTTCAGTAAATTATTCCGGTGACAATTTTTCGAACCGCATTAGT- 5′ |
| 16-24uw | 5′-CCTTTAGAGAAGTCATTTAATTTCCGGTGAGTTAAAAAGCTTGGCGTAATCA- 3′<br>3′-AGCCATGGGCCCTAGGAAATCTCTTCAGTAAATTATTCCGGTGACAATTTTTCGAACCGCATTAGT- 5′ |
| 9-24uw | 5′-CCTTTAGAGAAGTCTAAATTATTCCGGTGAGTTAAAAAGCTTGGCGTAATCA- 3′<br>3′-AGCCATGGGCCCTAGGAAATCTCTTCAGTAAATTATTCCGGTGACAATTTTTCGAACCGCATTAGT- 5′ |
| 9-24mm 9-24uw | 5′-CCTTTAGAGAAGTCATTTAATAAGGCCACTGTTAAAAAGCTTGGCGTAATCA- 3′<br>3′-AGCCATGGGCCCTAGGAAATCTCTTCAGATTTAATAAGGCCACTCAATTTTTCGAACCGCATTAGT- 5′ |
| 7-24uw | 5′-CCTTTAGAGAAGAGTAAATTATTCCGGTGAGTTAAAAAGCTTGGCGTAATCA- 3′<br>3′-AGCCATGGGCCCTAGGAAATCTCTTCAGTAAATTATTCCGGTGACAATTTTTCGAACCGCATTAGT- 5′ |
| 7-24mm 7-24uw | 5′-CCTTTAGAGAAGTCATTTAATAAGGCCACTGTTAAAAAGCTTGGCGTAATCA- 3′<br>3′-AGCCATGGGCCCTAGGAAATCTCTTCTCATTTAATAAGGCCACTCAATTTTTCGAACCGCATTAGT- 5′ |

PAM. DNA sequences complementary to guide RNA are shown in red (Cognate).

**Table S5. List of guide-RNA used in all experiments and DNA targets used in single-molecule cleavage product release assay.**

| Description | RNA Sequences |
|---|---|
| guide-RNA (AsCpf1 & FnCpf1) | 5′-AAUUUCUACUCUUGUAGAUGAGAAGUCAUUUAAUAAGGCCACU-3′ |
| Modified guide-RNA for Cy5 labeling (AsCpf1 &FnCpf1) | 5′-AAUUUCUACUCUUGUAGAUGAGAAGUCAUUUAAUAAGGCCACU-3′ |
| Modified guide-RNA for Cy5 labeling (LbCpf1) | 5′-UAAUUUCUACUAAG*UGUAGAUGAGAAGUCAUUUAAUAAGGCCACU-3′ |
| guide-RNA (LbCpf1) | 5′-GUAAUUUCUACUAAGUGUAGAUGAGAAGUCAUUUAAUAAGGCCACU-3′ |

Thymine modification for Cy5 labeling. IDT code: /iAmMC6T/
*amino-modifier phosphoramidite for smFRET binding experiments. Functionally interchangeable with the above-mentioned thymine modification. IDT code :/iUniAmM/
RNA sequences with thymine modification or amino-modifier phosphoramidite were used for or smFRET experiments to study DNA interrogation ——————————————by Cpf1-RNA. RNA sequences complementary to the protospacer in a cognate DNA target are shown in red (Cognate). Unmodified guide-RNA for LbCpf1 has an extra G at the 5′ end, compared to the canonical guide-RNA of LbCpf1. This is due to the T7 Transcription limitation which is one of the most widely used methods for both in vivo and in vitro transcription.

| Description | DNA Sequences |
|---|---|
| 0/0 | 16 nucleotide biotinylated adaptor for surface immobilization<br>5′- CAGTCCTGCTGGTCGT-TCGGTACCCGGGATCCTTTAGAGAAGTCATTTAATAAGGCCACTGTTAAAAAGCTTGGCGTAATCA- 3′<br>3′-*-GTCAGGACGACCAGCA AGCCATGGGCCCTAGGAAATCTCTTCAGTAAATTATTCCGGTGACAATTTTTCGAACCGCATTAGT- 5′ |
| 6 | 5′- CAGTCCTGCTGGTCGT-TCGGTACCCGGGATCCTTTAGAGAAGTCATTTAATAAGCGGTGAGTTAAAAAGCTTGGCGTAATCA- 3′<br>3′-*-GTCAGGACGACCAGCA AGCCATGGGCCCTAGGAAATCTCTTCAGTAAATTATTCGCCACTCAATTTTTCGAACCGCATTAGT- 5′ |

Thymine modification for Cy3 labeling. *Biotin. PAM. DNA sequences complementary to guide RNA are shown in red (Cognate).

# S2. Additional details about materials and methods

**DNA targets for smFRET analysis of DNA interrogation.** Single-stranded DNA (ssDNA) oligonucleotides were purchased from Integrated DNA Technologies. ssDNA target and non-target (labeled with Cy3) strands and a biotinylated adaptor strand were mixed. Excess target strand was used to ensure near complete hybridization of non-target strand with the target strand. Upon surface immobilization of the assembled DNA target, any free target strand can be washed away because it does not contain biotin. The non-target strand was created by ligating two component strands, one with Cy3 and the other containing the protospacer region to avoid having to synthesize modified oligos for each mismatch construct. For schematics, see **SI Appendix, Fig. S1*A*.** Fully duplexed DNA targets but with a nick were also used. The oligonucleotide containing Cy3 is referred to as "Cy3 oligo" and is in part, complementary to a "biotin oligo". Hybridization of the two oligos results in a biotin-Cy3 adaptor, which has a 14 nt overhang complementary to the "target oligo" that contains the protospacer region. Finally, the non-target "oligo" complementary to the target oligo was used to complete the duplexed DNA target (**SI Appendix, Fig. S1*A***). DNA targets were prepared by mixing all of the four component oligos in the buffer containing 50 mM NaCl, 20 mM Tris-HCl (pH 8.0), which was then heated to 90° C followed by slow-cooling to room temperature over 3 hr. The mixing ratio of component oligos was 1:1:2:3 for Cy3 oligo: biotin oligo: target oligo: non-target oligo. An excess of target and non–target oligo was used to ensure that any Cy3 oligo detected on the surface is in complex with three other oligos. The Cy3 fluorophore is located 4 bp upstream of the protospacer adjacent motif (PAM: 5'-YTTN-3') and was conjugated via Cy3 N-hydroxysuccinimido (Cy3-NHS; GE Healthcare) to the Cy3 oligo at amino-group attached to a modified thymine through a C6 linker (amino-dT) using NHS ester linkage. smFRET experiments were done with both sets of DNA targets (with or without a nick) and no significant differences were found between them. **Table S1** shows all DNA targets used.

**Expression and purification of Cpf1.** The methods of Cpf1 protein expression and purification were adapted from a protocol described previously(7). Codon optimized Cpf1 gene sequence cloned into a bacterial expression vector (6-His-MBP-TEV-FnCpf1, a pET based vector) was cloned in house or purchased from GenScript. The vector was transformed into Rosetta (DE3) pLyseS (EMD Millipore) cells and cells were plated onto LB-Kanamycin agar plates and grown at 37 °C overnight. Single colony from the agar plates was then cultured overnight in 10 ml of SOC medium (Thermo Fisher Scientific). The overnight miniculture of Rosetta (DE3) pLyseS cells containing the Cpf1 expression construct were inoculated (1:500 dilution) into 4 liters of Terrific Broth (Sigma Aldrich) growth media containing 50 µg/ml Kanamycin. Growth media with the inoculant was grown at 37 °C in a shaker at 100 rpm until the cell density reached 0.2 OD600, at which point the temperature was lowered to 21 °C. Growth was continued and 6-His-MBP-TEV-Cpf1 protein expression was induced when cells reached 0.6 OD600 by addition of IPTG (Sigma) to 0.5 mM final concentration in the growth media. The induced culture was kept for 14–18 hr at 21 °C after which the cells were harvested by centrifugation at 5000 rpm for 30 min at 4 °C. The harvested cells were quickly stored at −80 °C until further purification.

The harvested cells were then suspended in 200 ml of lysis buffer (50 mM HEPES [pH 7], 2M NaCl, 5 mM $MgCl_2$, 20 mM imidazole) supplemented with protease inhibitors (Roche complete, EDTA-free) from Roche and lysozyme (Sigma Aldrich) and incubated at 4 °C for 30-45 minutes. After homogenization, cells were further lysed by sonication (Fisher Model 500 Sonic Dismembrator; Thermo Fisher Scientific) at 30% amplitude in 3 cycles of 2 s sonicate-2 s relax mode, each cycle lasting 1 min. Following lysis, cell solution was centrifuged at 15,000 ×*g* for 30-45 minutes, the cellular debris was discarded and the supernatant of lysate was collected. The clear lysate was then incubated at 4 °C with Ni-NTA slurry (Qiagen) for 45 min in a shaker at 30 rpm. The lysate with the Ni-NTA slurry was then applied to a column and multiple cycles of lysis buffer were used to wash the Ni-NTA slurry through the column. The 6-His-MBP-TEV-Cpf1 was eluted in a single step with 300 mM imidazole buffer (50 mM HEPES [pH 7], 2

M NaCl, 5 mM $MgCl_2$, 300 mM imidazole). TEV protease (Sigma Aldrich) was then added, and the sample was dialyzed using Slide-A-Lyzer™ dialysis casettes (Thermo Fisher Scientific) overnight into the buffer suitable for TEV protease activity (500 mM NaCl, 50 mM HEPES [pH 7], 5 mM $MgCl_2$, 2 mM DTT). TEV protease activity resulted in the deconstitution of 6-His-MBP-TEV-Cpf1 into 6-His-MBP and Cpf1, which was confirmed by SDS-PAGE. The free 6-His-MBP was removed by another round of Ni-NTA chromatography resulting in the solution containing only Cpf1. Sample was then injected on to a HiLoad 26/600 S200 size exclusion column equilibrated with gel filtration buffer (50 mM Tris-HCl pH 8.0, 100 mM NaCl, 10 mM $MgCl_2$, 5mM DTT). Fractions containing Cpf1 were pooled, concentrated, and then flash frozen in liquid nitrogen. Final sample was stored at -80 °C until used in experiments.

**Single-molecule detection and data analysis.** NeutrAvidin-biotin interaction was used to immobilize the biotinylated Cy3-labeled DNA targets on the polyethylene glycol (PEG) passivated flow chamber surface prepared following protocols reported previously(9) or purchased from Johns Hopkins Microscope Supplies Core. Cy5-labeled Cpf1-RNA or unlabeled Cpf1-RNA (both referred to as Cpf1-RNA for brevity) was added to the flow chamber. The flow chamber was then illuminated with green laser and imaged with two color total internal reflection fluorescence microscopy. A buffer suitable for single-molecule imaging and Cpf1 activity was used and is referred to as the imaging-reaction buffer (50 mM Tris-HCl (pH 8.0) 100 mM NaCl, 10 mM $MgCl_2$,0.2 mg/ml Bovine serum albumin (BSA), 1 mg/ml glucose oxidase, 0.04 mg/ml catalase, 0.8% dextrose and saturated Trolox (>5 mM)) (SI Appendix, Fig. S18). 50 mM HEPES (pH 7.0) was used in place of 50 mM Tris-HCl (pH 8.0) for AsCpf1 experiments only, unless stated otherwise. 5 mM DTT was only added to these buffers for experiments done and stated to be in reducing conditions (chiefly LbCpf1 only). Technical details of single-molecule fluorescence detection, data acquisition and analysis have been described previously(9). Video recordings obtained using EMCCD camera (Andor) were processed to extract single molecule fluorescence intensities at each frame and custom written scripts were used to calculate FRET efficiencies. Data acquisition and analysis software

can be downloaded from https://cplc.illinois.edu/software/. FRET efficiency of the detected spot was approximated as FRET = $I_A/(I_D+I_A)$, where $I_D$ and $I_A$ are background and leakage corrected emission intensities of the donor and acceptor respectively. For single-molecule cleavage experiments, series of snapshots of different imaging areas were taken at different time points, under same green laser illumination via total internal reflection. The snapshots were then analyzed to estimate the changing number of Cy3-labeled DNA targets on the surface. Time resolution for all the experiments was 100 ms unless stated otherwise.

**Gel electrophoresis experiments involving visualization of nucleic acid bands via SYBR Gold II staining.** All experiments were conducted by mixing DNA targets and Cpf1-RNA in 1:5 ratio in the reaction buffer. The reaction was incubated for 4.5-5 hr (unless stated otherwise) before being resolved by 4% native/denaturing agarose gel electrophoresis and SYBR Gold II staining of nucleic acids using the precast gels containing SYBR Gold II, purchased from Thermo Fisher Scientific. For native gel electrophoresis, the reaction aliquots were directly loaded onto the gels. All the reactions were incubated at the room temperature, 37 °C or 4 °C and indicated in the presentation of their results. The gel electrophoresis was run at room temperature for experiments incubated at room temperature/37 °C and at 4 °C for experiments incubated at 4 °C. The cleaved-uncleaved DNA target with/without the bound Cpf1-RNA along with other nucleic acids were stained by SYBR Gold II and imaged by blue laser illumination (480 nm; GE Amersham Molecular Dynamics Typhoon 9410 Molecular Imager and 488 nm; Amersham Imager 600). For all of these experiments, the concentration of the DNA targets ranged from 20 nM to 60 nM and consequently the effective concentration of Cpf1-RNA ranged from 100 nM to 300 nM respectively. Volume of aliquots used for gel loading ranged from 10 to 20 μL per lane. For the time-lapse denaturing gel electrophoresis experiments, the acquired gel-images were quantified using ImageJ(10). Entire panel of DNA targets used in these gel-electrophoresis experiments is available in

**Table S3** and **S4**. Tris-HCl at pH 8.0 was used in the reaction buffers for all the experiments except for the ones reported in ***SI Appendix*, Fig. S2** and ***SI Appendix*, Fig. S9** where Tris-HCl at pH 8.5 was used.

**REFERENCES**


1. Yamano T, et al. (2016) Crystal Structure of Cpf1 in Complex with Guide RNA and Target DNA. *Cell* 165(4):949–962.

2. Dong D, et al. (2016) The crystal structure of Cpf1 in complex with CRISPR RNA. *Nature* 532(7600):522–526.

3. Stella S, Alcón P, Montoya G (2017) Structure of the Cpf1 endonuclease R-loop complex after target DNA cleavage. *Nature* 546(7659):559–563.

4. McKinney SA, Joo C, Ha T (2006) Analysis of Single-Molecule FRET Trajectories Using Hidden Markov Modeling. *Biophys J* 91(5):1941–1951.

5. Lee W, von Hippel PH, Marcus AH (2014) Internally labeled Cy3/Cy5 DNA constructs show greatly enhanced photo-stability in single-molecule FRET experiments. *Nucleic Acids Res* 42(9):5967–77.

6. Jiang F, et al. (2016) Structures of a CRISPR-Cas9 R-loop complex primed for DNA cleavage. *Science* 351(6275):867–71.

7. Zetsche B, et al. (2015) Cpf1 Is a Single RNA-Guided Endonuclease of a Class 2 CRISPR-Cas System. *Cell* 163(3):759–771.

8. Fonfara I, Richter H, Bratovič M, Le Rhun A, Charpentier E (2016) The CRISPR-associated DNA-cleaving enzyme Cpf1 also processes precursor CRISPR RNA. *Nature* 532(7600):517–521.

9. Roy R, Hohng S, Ha T (2008) A practical guide to single-molecule FRET. *Nat Methods* 5(6):507–516.

10. Schneider CA, Rasband WS, Eliceiri KW (2012) NIH Image to ImageJ: 25 years of image analysis. *Nat Methods* 9(7):671–5.